29506-6004-RU-00

Final Report

STUDY OF THE RELATION BETWEEN Pc 3 MICROPULSATIONS AND MAGNETOSHEATH FLUCTUATIONS AND OF THE MULTISATELLITE, MULTIMEASUREMENT INVESTIGATION OF THE EARTH'S BOW SHOCK

Contract No. NASW-2877

with

National Aeronautics and Space Administration
Washington, D.C.

30 December 1976

Space Sciences Department

TRW Defense & Space Systems Group
One Space Park
Redondo Beach, California 90278

TABLE OF CONTENTS

INTRODUCTION

This year's phase of the subject study concentrated heavily on completion of selected projects left over from the preceding year, including several publications with their myriad of time-consuming details of presentation and revision. Nevertheless, two new tasks were initiated of which one was finished and a report published. Both of these tasks involved the application of previous results in fresh contexts; they are described below in the section on Results. Also described below is the progress made in correlation of micropulsation with interplanetary magnetic field orientation. Reports are listed separately, of which the newest are attached as Appendices, following the Recommendations Section.

RESULTS

Micropulsations. The relationship between the direction of B_{SW} and the occurrence of Pc 3,4 micropulsations required by the postulated model was demonstrated. The previous Soviet results were tested and found to be largely verified, with the exception that where the Russians drew a distinction between Pc 3 and Pc 4, this study found that both bands follow essentially the same behavior. These findings, including the exception, are in substantial agreement with those of a recent thesis investigation by Gerard Nourry. The first report on this study's preliminary results for one station and one month's data (Calgary, September 1969) is awaiting publication by J. Geophys. Res. The report is attached to this report as Appendix 1.

The remaining available data from Calgary for October and November 1969 were added to the September data to enlarge the data base. The combined data were examined in scatter plot format. The results confirmed the preliminary conclusions from September data alone and emphasized the importance of low geomagnetic activity in exposing the correlation of elevated Pc 3 and Pc 4 amplitudes with low θ_{XB} (i.e., with $\underset{\sim}{B}_{SW}$ alignment with the solar wind). A report is in preparation.

An improvement in methodology was undertaken in which a computer program was about 50 percent completed that will aid in statistical analysis of the interplanetary field samples, eliminating the need to rely on the very crude $\theta_{XB(min)}$ employed so far.

Shock Structure. One accomplishment in this area was submission, review, and acceptance by J. Geophys. Res. of a detailed report on the quasi-parallel bow shock, appended in draft form to the final report of the preceding year's study. This paper gave the first observational description of a quasi-parallel structure in a plasma parameter regime which neither laboratory nor theoretical investigations had explicitly penetrated before.

Meanwhile, an opportunity arose to examine the shock in a very different guise. Virtually at the opposite extreme from the q-parallel structure is the sharp, narrow shock profile which occurs when the bow shock is nearly perpendicular. Several examples of extraordinarily thin shock crossings were found in the OGO-5 magnetometer record by Formisano, which he interpreted as representing truly perpendicular shocks. On examination of the upstream field, however, the shocks were found to be quasi-perpendicular, although only by about 10-20° (i.e., $\theta_{nB} \approx 70\text{-}80°$). Also, their unusual thinness could be interpreted as consistent with the marginal stability criterion applied to wholly different, laminar, cases by Morse and Greenstadt (1976). The first of the two "new" tasks mentioned in the Introduction was to examine these shocks, using the approximation adopted by Morse and Greenstadt (1976) to estimate the thicknesses of the thin, nearly perpendicular bow shocks at supralaminar Mach numbers. The accompanying figure in Appendix 2 shows the comparison of calculated and experimentally derived shock thicknesses extended to the range of Formisano's cases. Unfortunately, the apparent harmony of the figure is dependent on the values chosen for a number of experimental, or experimentally-inferred, parameters used to estimate the "observed" shock thickness (abscissa). The best interpretation and the best

way of presenting the thin shock cases is still unresolved as this is written, so no final result can be cited. If the relationship of the figure proves acceptable, then a major extension of the marginal stability criterion will have been achieved.

The second "new" task dealt with the foreshock. In a follow-up of an investigation recently published, with input from this study, by Diodato et al. (1976), an effort was made to develop the simplest implied relations between waves and particles upstream from the bow shock. In this initial project, the statistical results of Diodato et al. were translated into the guiding center energies of return protons as they might appear to a solar wind particle detector, such as that of ALSEP, looking in the appropriate direction. A report on the outcome has been published by GRL. The report is attached as Appendix 3. This result is related to a study of the ALSEP data begun recently by Benson (Rice) and is also related to the need for compiling information helpful in guiding the ISEE data analysis. With this in mind, a more comprehensive attack was initiated on the relationship between the energy spectrum of particles reflected at the shock and of return particles as they might be observed at a distant location upstream.

REPORTS

Reports Published

A statistical study of the upstream wave boundary outside the earth's bow shock, by Diodato, Greenstadt, Moreno, and Formisano, J. Geophys. Res., 81, 199, 1976.

Thickness of magnetic structures associated with the earth's bow shock, by Morse and Greenstadt, J. Geophys. Res., 81, 1791, 1976.

Energies of backstreaming protons in the foreshock, by Greenstadt, Geophys. Res. Lett's., 3, 553, 1976.

Reports in Press

Structure of the quasi-parallel, quasi-laminar bow shock, by Greenstadt, Russell, Formisano, Hedgecock, Scarf, Neugebauer, and Holzer, J. Geophys. Res.

Pc 3,4 activity and interplanetary field orientation, by Greenstadt and Olson, J. Geophys. Res.

RECOMMENDATION

The results obtained in this study (Appendix 1), combined with the earlier ones of Soviet researchers and more recent ones by Webb and Orr (1976), Nourry (Ph.D. thesis), and Arthur and McPherron (1976) lend weight to the existence of a PCSO phenomenon ("Continuous Pulsations of Shock Origin," see Appendix 1) that spans the Pc 3,4 separation at 45 seconds' period and behaves, under quiet conditions, in a manner consistent with the model of such a phenomenon proposed by this investigator. The stage is set therefore for the refinements and developments needed to proceed to a quantitative expression of the connection between the IMF and surface activity. Two endeavors should head a list of follow-on efforts. One is a program of "combing" through the statistics of space and surface measurements to discover the most potent conditions for transfer of PCSO between the solar wind and

the ground; the second is a focused attempt to find particular cases in which, through multiple observations, connected events in the solar wind, magnetosheath, outer and surface magnetosphere can be discovered and described.

Study of shock structure itself has progressed to a point at which the macrostructure is moderately well described, if not understood, while the microstructure requires new, high-resolution measurements for thorough comprehension. The most fruitful areas of investigation in the near future seem to be the following:

1. Theoretical examination of the quasi-parallel structure, now that the firehose mechanism has been found to be unlikely in one case (Greenstadt et al., 1976);
2. Advance preparation for the refined measurements of ISEE, by developing estimates of parameters of particle and field behavior in the shock and foreshock, as in Appendix 3, i.e., prepare to test present knowledge against pending observations;
3. Comparison of existing theoretical models against the highest resolution observations currently available, to determine anomalous resistivity, for example, or to compare observed with predicted acoustic noise levels.

It is recommended that study of the solar wind-bow shock-magnetosphere interaction from the plasma physics viewpoint be pursued further, with increasing attention to quantitative estimates and theoretical comparisons along the lines outlined above.

REFERENCES

Arthur, C. W., and R. L. McPherron, The interplanetary magnetic field associated with synchronous orbit observations of Pc 3 magnetic pulsations, UCLA IGPP Publication No. 1610, submitted to J. Geophys. Res., 1976.

Diodato, L., E. W. Greenstadt, G. Moreno, and V. Formisano, A statistical study of the upstream wave boundary outside the earth's bow shock, J. Geophys. Res., 81, 199, 1976.

Greenstadt, E. W., C. T. Russell, V. Formisano, P. C. Hedgecock, F. L. Scarf, M. Neugebauer, and R. E. Holzer, Structure of the quasi-parallel, quasi-laminar bow shock, J. Geophys. Res., in press, 1976.

Morse, D. L., and E. W. Greenstadt, Thickness of magnetic structures associated with the earth's bow shock, J. Geophys. Res., 81, 1791, 1976.

Nourry, G. R., Interplanetary magnetic field, solar wind and geomagnetic micropulsation, Thesis, Univ. of British Columbia, Dept of Geophysics & Astronomy, 1976.

Webb, D., and D. Orr, Geomagnetic pulsations (5-50 mHz) and the interplanetary magnetic field, J. Geophys. Res., in press, 1976.

APPENDIX 1

Pc 3,4 ACTIVITY AND INTERPLANETARY FIELD ORIENTATION

E. W. Greenstadt

Space Sciences Department
TRW Defense and Space Systems
Redondo Beach, California 90278

J. V. Olson

Institute of Earth & Planetary Physics
University of Alberta
Edmonton, Alberta, Canada T6G 2J1

1 April 1976

Short Title: IMF DIRECTION AND PC 3-4

Space Sciences Department

TRW Defense and Space Systems
One Space Park
Redondo Beach, California 90278

Pc 3,4 ACTIVITY AND INTERPLANETARY FIELD ORIENTATION

ABSTRACT

Examination of Pc 3,4 micropulsation waveforms recorded at Calgary in the interval 2-20 September 1969 shows a tendency for signal enhancement to have occurred when the interplanetary magnetic field made a small angle θ_{XB} with the sun-earth line. Scatter plots of hourly Pc 3,4 amplitudes show a definite trend toward large signals when $\theta_{XB} < 50\text{-}60°$ and a corresponding disappearance of significant amplitudes when $\theta_{XB} > 60°$, but there was appreciable variability in individual cases. The trend toward the highest amplitudes when $\theta_{XB} \approx 0°$ was sharpened under geomagnetically quiet conditions. Power density spectograms improved the correlation of pulsation strength with low angle in some cases. The results are interpreted as compatible with enhanced probability of Pc 3,4 excitation when quasi-parallel structure prevails at the subsolar point of the bow shock and consistent with previous Soviet and Canadian analyses, although certain details of the Russian results are not supported.

INTRODUCTION

Successful use of magnetic fluctuations, including micropulsations of the earth's surface field, as indirect diagnostics of magnetospheric and solar wind conditions is of capital importance for two reasons: First, accurate empirical coupling of surface with exospheric and heliospheric parameters would open the path to a quantitative theoretical description of the entire magnetospheric transfer function; second, surface diagnostics would be considerably thriftier than the continuous deployment of satellites for direct measurements.

The subject of magnetic diagnostics is as old as the inference that magnetic storms are initiated by corpulscular emissions from the sun and as new as the inference that magnetic substorms are initiated by southward-oriented interplanetary magnetic field (IMF). Recently, attention has been directed to some remarkable correlations between micropulsation characteristics in the 10 to 150-sec period range (Pc 3,4) and solar wind parameters (Troitskaya et al., 1971; Gul'yel'mi et al., 1973; Plyasova-Bakunina, 1972). One such correlation is manifested in the preferential appearance of Pc 4 when the interplanetary field vector $\underset{\sim}{B}_{SW}$ points either sunward or antisunward, i.e., parallel or antiparallel to the solar ecliptic X-axis and, conversely, in the preferential disappearance of Pc 4 when $\underset{\sim}{B}_{SW}$ is in or close to the solar ecliptic Y-Z plane, i.e., orthogonal to X (Bol'shakova and Troitskaya, 1968; Nourry and Watanabe, 1973).

At the same time the early versions of this correlation were being asserted, the foundation for a qualitative model predicting the same correlation was being laid by disclosure of the time-varying, field-dependent

pulsation (now called quasi-parallel) structure of the earth's bow shock (Greenstadt et al., 1970; Greenstadt, 1972a). The resulting model postulated that the time-varying appearance of the daytime micropulsations Pc 3,4 might be triggered and maintained by the propagation or convection of large amplitude, quasi-parallel shock oscillations through the magnetosheath to the magnetopause (Greenstadt, 1972b). The model suggested that alignment of $\underset{\sim}{B}_{SW}$ with the solar wind flow, hence essentially with X and therefore parallel to the nominal shock normal at the subsolar point, would furnish the most favorable circumstance for transferring quasi-parallel oscillations through the thinnest part of the magnetosheath to the subsolar portion of the magnetopause. Daytime micropulsations would thereby be excited on the magnetospheric field lines rooted at auroral latitudes where Pc 3,4 have the largest amplitudes. Again, the model suggested the converse as well: namely, that orthogonality of $\underset{\sim}{B}_{SW}$ and X should remove all areas of quasi-parallel structure to the flanks of the bow shock, producing the least favorable conditions for transfer of oscillations to the subsolar magnetopause and therefore leaving Pc 3,4 unstimulated, at least by this postulated mechanism.

The investigation whose initial outcome is reported here was undertaken to test the model described above and to extend the earlier correlational studies by introducing spectral analysis of the micropulsation records. Previous use of power spectral technique for establishing these correlations has not been published.

Our results so far are positive, butpertain to a relatively small sample and are compromised by considerable ambiguity. Nevertheless, the apparently strong positive correlation asserted by other workers justifies careful examination of even a limited data set. After all, the value of a

diagnostic is highest when it applies not only to small samples but to individual cases, and individual cases have been emphasized in earlier studies (Bol'shakova and Troitskaya, 1968; Nourry and Watanabe, 1973). Although this is a continuing study, we think it valuable nevertheless to pause and convey these preliminary findings to those concerned with micropulsation diagnostics. In the following section we describe the sources of data so far examined, the processes to which they have been subjected, and the rationale by which examples were selected for this report. We then display some examples and discuss the outcome at this stage of the investigation.

DATA SOURCES AND PROCESSES

Sources. The last four months of 1969 offered an interval in which all the magnetometers of the meridional chain of the University of Alberta were recording field fluctuations a substantial fraction of the time, while lunar orbiter Explorer 35 provided almost continuous coverage of the interplanetary (solar wind) field B_{SW}, exclusive of the monthly transit of the moon through the dusk-to-dawn magnetosheath and magnetotail and the brief periodic-eclipses of the satellite by the moon. In total, three subintervals of approximately 18 continuous days each in September, October and November 1969 were open to inspection. We report here on the September 2-20 interval and the data obtained by the Calgary magnetometer and the NASA/Ames research center (ARC) magnetometer aboard Explorer 35. Data from the remaining months are currently under analysis and appear to confirm the basic properties of the September sample.

Satellite data handling. The NASA/ARC magnetometer and data system characteristics have been described in the literature (Mihalov et al., 1968). For our purpose, the average of each sequence taken over 82 seconds containing 13 or 14 vector samples in the pattern 13,13,14,13,13,14,..., was used to compute

the angle θ_{XB} between X and $\underset{\sim}{B}_{SW}$ and plotted on common time scales with various representations of Pc 3,4 behavior.

Micropulsation data handling. The University of Alberta magnetometer stations are equipped with identical triaxial fluxgate magnetometers and digital recording equipment. The recordings represent vector samples taken at 1.92-second intervals. The instruments are described in Samson et al. (1971). The magnetometer station near Calgary, Alberta is located at 51°10'N, 114° 30'W geographic; 58.4°N, 302.9°E centered dipole. Local noon is at 19.67 UT.

The data were treated first by filtering them into Pc 3 and Pc 4 bands and displaying them as filtered waveforms. The three data axes were labeled X, Y and Z and represent the magnitudes of the local magnetic north, east and downward components of the field respectively.

Next, the data were filtered in a broad band and divided in time segments; power spectra were computed; and digital displays were printed out in sonogram form. As the data were read from the data tape they were bandpass filtered to include frequencies between 0.001 Hz and 0.0326 Hz (periods between 1000 seconds and 31 seconds). The filter operation was accomplished using simple recursive filters which resulted in a 6-db/octave amplitude decrease outside the above-mentioned frequency band. A subsequent pass through the data was made to cover the frequency band from 30 seconds to the 4-second Nyquist period.

Each line in the resulting digital sonograms represented the spectrum calculated over a 16-minute and 23.0-second interval. Each subsequent line is updated by half of this interval, or 8 minutes and 11.5 seconds. Thus,

each line in a sonogram represented a spectrum from an interval which overlapped the preceding and the following intervals. Every other spectrum was an independent spectrum.

Once computed, a spectrum was quantized into 10 levels. For all of the spectra the limits were set at $10^{5}\gamma^{2}/Hz$ and $10^{-1}\gamma^{2}/Hz$. From the base level, each subsequent level was 6 db or a factor of 3.981 times as large as the last.

The output sonograms, or spectrograms, appeared in the form of listings on ordinary printout forms, which were difficult to interpret in terms of patterns of activity. Overlays were therefore made on which symbols representing the various power levels were inscribed by hand.

Intrinsic ambiguity. A certain amount of ambiguity is unavoidable in the analysis procedure. First, there is the statistical preference of $\underset{\sim}{B}_{SW}$ for the average 45° stream angle in the ecliptic, midway between the aligned ($\theta_{XB} = 0$) and orthogonal ($\theta_{XB} = 90°$) cases that are expected to definitively control micropulsation behavior. Incidents of statistically unorthodox field orientations are therefore required to obtain any clear-cut correlation, so that the majority of data comparisons are likely to be indeterminate. A second difficulty centeres on the relatively frequent rate at which $\underset{\sim}{B}_{SW}$ fluctuates about its average direction, because the time between changes can be comparable to the delay between the change crossing a given interplanetary observation point and the arrival of that change at the earth. If we want to relate changes in micropulsation occurrence on the surface to changes in θ_{XB}, we must either (a) know the correct delay at all times, (b) confine the investigation to intervals of

isolated change in θ_{XB} whose postulated consequences, if they exist, would be easily identifiable, or (c) work only on a compressed time scale where the anticipated delays would be insignificant. The first solution, i.e., full knowledge of all delays, was impossible, so we depended on the other two (b) and (c). The delay problem is described further in a later section.

DATA PRESENTATION

Waveforms. Figure 1 contrasts the only two days of stable, but opposing conditions in the September period. The daytime intervals of 2 and 19 September are shown on a very compressed time scale, displaying θ_{XB} and one axis of the filtered Pc 4 band only. The 51° line across the θ_{XB} panel denotes the nominal angle above which the subsolar point of the bow shock is changed from quasi-parallel to quasi-perpendicular structure. That is, there should be no oscillatory structure at the vertex of the bow shock when $\theta_{XB} >$ 51°. This angle was derived using pulsation parameters p = 1.6 (Greenstadt, 1972c; Diodato et al., 1976).

An overall contrast in micropulsation activity between the two days' records is evident, and we see considerable variability in wave amplitude on 19 September. We also see what amounted to a cutoff, or at least a substantial decrease, in Pc 4 signal at about 2220 even though no extraordinary shift in θ_{XB} occurred then, and we see an enhancement in Pc 4 at about 2330 even though θ_{XB} was higher then than at 2220. Thus, the gross correlation of θ_{XB} with overall Pc 4 activity for contrasting days was not supported by a one-for-one time correlation in the waveform representation. These onsets and cutoffs do not appear to have had any connection with the 51° value of θ_{XB}.

Additional examples showing θ_{XB} behavior more typical of the interplanetary field are displayed in Figure 2. The six examples each cover the three hours before and after local noon and present both filtered Pc 3 and Pc 4 bands. Gaps in the ground signal have been introduced to correspond to gaps in the spacecraft data, since occasional amplitude changes during such gaps were found to be visually distracting. The examples are in chronological order (a) through (f), and clearly show the midvalue preference and high variability of θ_{XB}.

Every combination from correlation to anticorrelation appears in Figure 2. Correlations, when they occurred, were always visible principally in the horizontal plane at Calgary, i.e., along the X and/or Y magnetometer axes. This property is consistent with the linear or high-eliplicity polarizations of Pc 3,4 (Arthur et al., 1973; Fukunishi and Lanzerotti, 1974). For the figure we selected whichever axis showed more activity or the better correlation.

Making allowance visually for possible small time displacements between satellite and earth, Figures 2(c) and (f) give the strongest appearance among the six panels of correlation in both Pc 3 and 4 channels. Certainly the largest signals correspond to the θ_{XB} in the upper half of its panels and vice versa. Changes in signal amplitude concurred, more or less, with swings in θ_{XB}, but these were generally too rapid and too extreme to confirm or contradict the validity of the division at 51° or any other particular value.

Correlation of Pc 4 with θ_{XB} in 2(e) is subtle at best, and Pc 3 and 4 amplitude patterns are not nearly so similar to each other as in (c) and (f).

In (b), the Pc 3 and 4 signals are also dissimilar but it was Pc 3 that followed the θ_{XB} pattern in rough outline rather than Pc 4. In fact Pc 4 amplitudes were peaking in hours 21-23 in (b), contrary to the form suggested by θ_{XB}. Also in (b), the midvalue of θ_{XB} ($\approx 45°$) was a suitable candidate for separating more from less active Pc 3 signals. Note that in (e) the absolute amplitudes of Pc 4 were larger than those in (b) although θ_{XB} was almost always less favorable to micropulsations in (e) than in (b), according to the model.

The entire Pc 4 segment in (d) is indicative of noncorrelation everywhere, and even anticorrelation in some intervals, while there is little, if any, correlation to be seen in (a) between θ_{XB} and either Pc 3 or Pc 4 enhancements. There were some bursts in both channels in (a) which might have been related to brief excursions of θ_{XB} below 30°, but the general pattern of micropulsation amplitudes does not appear to have followed that of the field angle at all. The right-hand half of the Pc 3 record in (d) might be interpreted by an uncritical observer as suggesting correlation of signal amplitude with $\theta_{XB} \lesssim 30°$, given a generous time delay from spacecraft to earth, but the left half was certainly uncorrelated.

Taken as a whole, Figure 2 must be regarded as contributing substantial ambiguity to the attempt to document an association between θ_{XB} and Pc 3,4 activity, either through patterns of incidence or absolute values of micropulsation amplitude.

Scatter plots. Figure 3 condenses and summarizes in scatter diagram form the information contained in the low-resolution, band-filtered waveform plots, such as those of Figures 1 and 2, for the hours 1600-2400 UT in the interval 2-20 September 69 inclusive. The vertical scale represents the maximal peak-to-peak amplitude during each hour of micropulsation data; the horizontal scale gives the smallest angle reached by θ_{XB} during the same hour. Hours with less than three-quarters complete recording at either Explorer or Calgary were omitted. Points representing the Pc 3 band are in the three upper panels, points representing the Pc 4 band are in the three lower panels. In each graph, histograms have been drawn of the highest and lowest amplitude recorded in every five-degree interval 0-4°, 5-9°, etc. Intervals in which no points occurred are traversed by dashed lines.

The two leftmost graphs, (a) and (d), contain all the data from the respective micropulsation channels. The "cross-flow" geometry, i.e., θ_{XB} roughly from 70° to 90°, corresponds to micropulsation activity essentially at the noise level of the Calgary instruments. Both channels show a definite increase of the range of recorded amplitude for decreasing θ_{XB}. The increase appears to have been caused by signals of substantial amplitudes up to an order of magnitude larger than background, clustered in two separate ranges of θ_{XB}: 20-50° and 0-10°. The most extreme excursions occurred for the 0-10° cases.

A partial ordering of the data was obtained by separating hours of no magnetic activity from hours of even modest geomagnetic storminess. This is seen in Panels (b),(c) and (e),(f). Essentially the entire group of Pc 3 amplitudes > 2 , and Pc 4 amplitudes > 3 , enclosed in the shaded boxes (less only one point in each

channel), that fell in the range θ_{XB} = 20-50° belonged to hours when $K_p \geq 2+$. Thus the groups of high amplitude cases in the 20-50° range disappeared from (b) and (e) when hours with disturbed field were excluded. The result, in (b) and (e), is that under quiet conditions the increase of the amplitude ranges still appears to have taken place in two stages, but these are defined differently: first, there was an increased incidence of signals above instrument threshold when $\theta_{XB} \lesssim 50°$, second, there were very large amplitudes when $\theta_{XB} \lesssim 10°$. In (b), this trend survived even the removal of the lone high point at 3°. Conversely, for $K_p \geq 2+$ in (c) and (f), wide ranges, including high levels, of amplitude occurred in a "bulge" between 20 and 50° (actually, 20-40° if we look at individual points rather than histograms), although these cannot be represented as increases above threshold because no large θ_{XB} values were associated with disturbed cases, where threshold might have been seen. Large amplitudes also occurred between 0 and 10° during disturbed hours.

The distinct scatter patterns obtained by the separation at $K_p = 2°$ changed slightly when the criterion of disturbance was altered; e.g., when the separation was made at $K_p = 2+$ (not shown) instead of $K_p = 2°$, the "quiet" division for $K_p \leq 2+$ reacquired two points of the 20-50° cluster and a few points in the 0-10° range, while the "disturbed" division for $K_p \geq 3-$ lost substantial population in its 0-4° maximum. These shifts applied to both Pc 3 and Pc 4 channels. We obtained the impression that, allowing for uncertainty in the meaning of individual points and for the inherent ambiguities discussed earlier, undisturbed intervals tended toward the "two-stage" pattern already described, and disturbed intervals tended to consist of a pattern of large amplitudes for the middle θ's and a range of moderate amplitudes for low θ's, not necessarily including a zero-peak.

Spacecraft geometry. Our overall interpretation of the results will be set forth in the Discussion, but we must preface the next few paragraphs of data presentation by noting that one source of scatter and imprecision in the plots of Figure 3 could have been poor time coordination. The compressed time scale of Figures 1 and 2 serves to minimize the possible uncertainties in delay from spacecraft to earth. But of many factors that might influence either a physical correlation of interplanetary field direction with micropulsation activity or the ability to demonstrate such a correlation is the unavoidable time lapse between a change in θ_{XB}, which must be measured outside the bow shock, and a (hypothetically) consequent micropulsation event on the earth's surface. Either phenomenon could occur before the other, with the delay and the sequence depending on solar wind conditions and on the location of the interplanetary observation point.

In the interval discussed here, involving Explorer 35, the spacecraft-earth geometry is shown in solar ecliptic projection in Figure 4. Four representative spacecraft-to-earth delays, neglecting magnetospheric transmission, are labeled in the figure: three corotation delays for average 45° stream angle (+30, zero, and -30 minutes) and one direct convection delay for average solar wind velocity (+19 minutes). The figure shows that half-hour time displacements, positive or negative, were to be expected during the 20-day interval being reported, and other field configurations giving almost arbitrary displacements could easily be imagined. Indeed, since field direction and its variation are at the very core of this investigation, varying geometry and varying delays were doubtless implicit in the data profiles.

Moreover, the longer delays, say 20 minutes or more, tended to be of the same timescale as the longevity of typical interplanetary field configurations themselves. It was therefore necessary to be highly selective in examining data with greater time resolution, but it was desirable to do so because this was the approach employed by earlier investigators.

High resolution waveforms. To examine the θ_{XB}-Pc relationship on an expanded time scale, we selected the two days, 7,8 September, bracketing the time of zero nominal corotation delay indicated in Figure 4. We reasoned that the relative positions of Explorer 35 and earth should have restricted the delay to no more than $\approx$ +15 minutes for that geometry. The data surrounding local noon on 7 and 8 September are shown in Figure 5. Here, bandpass filtered data from all three axes of the surface magnetometer were plotted for completeness.

In Figure 5(a), the field rotated from unfavorable to favorable angles during the four-hour interval depicted, but there does not appear to have been any corresponding increase in micropulsation activity. Indeed, the amplitude of Pc 4 noise was lower after 2020 than before, although the most favorable field directions indicated by the earlier figures were first established at that time. There was obviously no clear cutoff of signals in Figure 5(a) when $\theta_{XB} > 51°$.

Figure 5(b) shows that the field direction was never particularly favorable to Pc 4 during the midday interval of 8 September, but bursts of oscillations of amplitude larger than any recorded on the previous day [Figure 5(a)] were detected anyway. There is a mild suggestion in Figure 5(b) that

the bursts of micropulsations occurred when θ_{XB} dropped to about the 50° level. Nonetheless, oscillations in the X-component at Calgary were clearly present around 1840-1915 when θ_{XB} was in the range 70-90°, and it is unclear whether the 8 September case should be viewed more as example or counter-example of the relationship whose validation is the object of this study.

Spectrograms. A second source of uncertainty in individual cases and scatter in statistical summaries could have been varying spectral content of the micropulsation signals. The maximum amplitude of signal enhancement during an hour of the very compressed time scale we used to construct the plots of Figure 3 could have been produced by micropulsation wavetrains anywhere in the Pc 3 or Pc 4 bands. However, the main property of Pc waves that has always excited attention is their often, almost monochromatic, or at least band-limited appearance. Since natural noise declines in amplitude, and power, with frequency (Santirocco and Parker, 1963; Jacobs, 1970), i.e., $P \propto f^{-\alpha}$, one excursion of θ_{XB} to 0° could have been associated with a wavetrain of narrow frequency content at the low end of the Pc 4 band while a similar excursion in another hour could have been associated with a wavetrain of lesser amplitude at the high end of the Pc 4 band. Both events could have been "correlated" yet appear far apart in amplitude on a scatter plot. Furthermore, short-lived pulsation events (bursts) could have distorted the amplitude statistics since they might not have represented the overall state of micropulsation activity during the interval in which they fell. To overcome these

sources of difficulty and introduce more objectivity into the analysis that has tended to rest on visual assessment of micropulsation activity, we introduced the use of spectrograms. The spectrogram format displays the general features of pulsation activity throughout an interval without restricting the display to a particular frequency band in searching for correlations. Also, the effects of spikes or short-lived pulsations are minimized, so the spectrogram format emphasizes persistent features of the micropulsation train.

Figure 6 contrasts the two "favorable" and "unfavorable" days whose waveforms were shown in Figure 1. The format of each remaining spectral figure consists of an upper panel showing θ_{XB}, with the angle increasing toward the bottom, and a lower panel showing Pc 3-4 spectrograms, with period increasing toward the bottom. The intervals illustrated cover data acquired during local daytime at Calgary. A break in the surface data in Figure 6(a) is used to display the symbols employed to represent different levels of spectral power at any given point of the t,T coordinate system, where t is time and T signifies pulsation period.

Figure 6(a) shows that during the daytime pass of 2 September 69 at Calgary, when the interplanetary field was rarely less than 60°, and usually more than 70° from the sun-earth line, micropulsation activity was never above 6.3 γ^2/Hz for any period, was usually below 1.6 γ^2/Hz, and was often less than .4 γ^2/Hz. Figure 6(b), on the other hand, shows that on 19 September, when B_{SW} was rarely more than 30°, and usually less than 20° from the sun-earth line, micropulsation activity was commonly above 6.3 γ^2/Hz, often above 25 γ^2/Hz, and occasionally above 100 γ^2/Hz in the Pc 4 band. More often than not the power density was above 1.6 γ^2/Hz throughout the Pc 3-4 range.

Figure 6 certainly suggests gross correlations between low θ_{XB} and elevated Pc 3-4 power or, conversely, between high θ_{XB} and depressed Pc 3-4 power. This suggestion is reinforced by the data of Figure 7, where during the most favorable local prenoon observing hours on 11 September, θ_{XB} gradually shifted from the 10-40° range to the 60-90° range, accompanied by a decline in average spectral density of Pc 4.

It can be seen that there are a few horizontal strings of symbols in Figures 6 or 7 that could represent narrowband or nearly monochromatic pulsation signals persisting for long intervals, so that when the noise level increased it certainly did not always fill the entire Pc 3 or Pc 4 range at any fixed value. The highest amplitude signals were often grouped into period intervals appreciably narrower than the full micropulsation bands. Moreover, the maximal power density occurred at different periods at different times. This "clumping" property visible in the spectra bears directly on the interpretation of whether or not field direction and pulsation activity correlate in specific cases. Thus the visual impression made by a single set of data, and the interpretation derived therefrom, can depend heavily on whether waveforms or spectrograms are examined.

Two examples in which spectra give more positive results than waveform inspection are shown in Figure 8. The Pc 4 waveforms in the portion of 8(a) from 1800 to 2200 were shown in detail in Figure 5(a) and described as essentially ambiguous with regard to the correlation with angle. In 8(a), however, there is an indication that the pattern of increased pulsation activity followed the trends of θ_{XB} toward 0°, with the exception of the sudden decline in Pc 4 power at 2100. In so interpreting the spectral pattern, it is necessary to take into account all enhancements of the spectral density regardless of period, which clearly varied from event to event. There does appear to have been a delay of about 20 minutes from spacecraft to earth in 8(a) despite the selection of 7 September as a day of potentially zero delay. This example therefore illustrates the ubiquity of unknown time shifts as a source of inherent ambiguity in this type of study.

Figure 8(b) is the spectral version of the waveform example of Figure 2(d), which was described earlier as showing a substantially uncorrelated or anticorrelated result in the Pc 4 channel. This view is not sustained by examination of 8(b), where Pc 4 activity appears to have been strongly correlated with decreases in θ_{XB} provided only that we do not require all bursts of activity to occur at the same period. For example, the sudden swing of θ_{XB} close to 90° (above 51°?) at about 1814 was accompanied by a cutoff of broad Pc 3 and 4 activity, but the return of θ_{XB} to middle values was accompanied by the enlargement of Pc 4 noise only close to the long-period edge of the band.

Figure 8(b) also illustrates an important property of the pulsation activity revealed by the spectra generally: as a rule, strong Pc 3 activity, say above the 6.3 γ^2/Hz level, appeared as an extension of stronger activity of longer period in the Pc 4 band which seemed to "spill over" into the Pc 3 range. Thus, we found little or no indication of any separate Pc 3,4 phenomena. There appeared to be a single band from T = 20 to 150 seconds whose power spectrum consisted either of one or more band-limited maxima or a decline with frequency that rose and fell as a whole from one time to another.

In sum, the spectrograms tended to increase confidence in the indications of positive correlation by demonstrating the disadvantage of treating the Pc 3,4 bands either as separate or uniform units. Unfortunately, we have

not, at the time of writing, succeeded in devising a means of condensing the three-dimensional information content of the spectrograms (nine-dimensional, if all three axes are to be studied) into a satisfactory format in which the whole body of data can be compared at a glance. We did determine that the straightforward preparation of the scatter plots of Figure 3 probably give a more reliable synopses of Pc 3,4 properties than an attempt to interpret, or seek "events" in expanded waveforms such as those in Figure 5, could have done.

SUMMARY OF RESULTS

The waveform data, as displayed in the accompanying figures, fell short of providing clear proof for a one-for-one correlation of low θ_{XB} with high Pc 3 or 4 incidence on an event-by-event basis. However, the scatter plots derived from hourly data plotted on a highly condensed time scale supported the existence of a trend compatible with a positive correlation. We interpret the plots of Figure 3 to indicate that the

probability of occurrence of both Pc 3 and Pc 4 events of appreciable amplitude was much higher when θ_{XB} was close to 0° than at any other orientation and significantly higher for $\theta_{XB} \lesssim 60°$ than for $60° \lesssim \theta_{XB} \lesssim 90°$. The wide scatter amplitudes for $\theta_{XB} \lesssim 50\text{-}60°$ and the failure of strong correlation to appear in individual cases suggests that factors other than θ_{XB} (including methodological ones) played an important role in determining micropulsation amplitudes at any given time. The trends of declining Pc 3,4 amplitudes with increasing θ_{XB} were clarified under undisturbed geomagnetic conditions, mainly by reduction of scatter for middle values of θ_{XB}. The scatter plots and spectrograms of the micropulsation records indicated that the division between Pc 3 and Pc 4 bands at $T = 45$ seconds was unimportant to this study. The spectograms were more favorable to correlation in individual cases than the waveforms, provided signal enhancements were given equal weight visually, independent of their periods.

DISCUSSION

Scatter. Two sources of scatter in the hourly summary plots of Figure 3, namely unknown satellite-earth delays and inconstant periodicities of band-limited wavetrains, have already been discussed and shown to have been plausible contributors to the wide ranges of Pc amplitudes associated with angles below $\theta_{XB} \approx 60°$. These factors do not exhaust the possibilities, however. A few others are:

1. Dwell time. The hourly $\theta_{XB(MIN)}$ values used here represented anything from 1-point transients to stabilized field orientations. There could be a minimal dwell requirement on θ_{XB} to produce elevated signal amplitudes. Also, low transient values of θ_{XB} may accompany fluctuating fields that have a compounding effect on the generation of micropulsations.

2. Longitude. All local daylight times before and after noon were combined. But magnetospheric transmission of, or resonant response to, micropulsation signals could be sufficiently dependent on local time to introduce serious uncertainties in undifferentiated compilations. Perhaps midday hours should be treated separately.

3. Variable delays. Minute-to-minute, inconstant transport times of changes in θ_{XB} from the upstream observation point to the magnetopause would enormously complicate any effort to compare events on a one-for-one basis. This difficulty would increase with satellite distance, and would be overcome by either a large statistical sample and/or use of data from a satellite much closer to the magnetopause than Explorer 35.

4. Sporadic validity. Plasma, i.e., solar wind, parameters are highly variable, particularly in the magnetosheath, and we consider it plausible

that correlation between θ_{XB} and Pc occurrence may be precluded or permitted under special intermittent circumstances involving the physical conditions for transfer of signals across the magnetopause (Gokhberg et al., 1971; Wolfe and Kauffman, 1975) or the superposition by the magnetosheath of its own noise spectrum caused by local instabilities.

5. Variable sources. There may be wholly separate mechanisms for generation of signals in the Pc 3-4 frequency range, as many workers believe, so that only a portion of the enhanced amplitudes observed were attributable to processes outside the magnetopause.

6. Ringing. Persistence of oscillations in the magnetosphere after the initial excitation at the magnetopause could have produced some of the scatter in Figure 3, falsely imputing high amplitudes to midvalues of θ_{XB} and perhaps exaggerating the apparent step at 50-60°.

All of the causes of imperfect correlation listed above can be overcome by statistical analysis of suitably-defined subsets of observations if the number of points in each subset is large enough. Further study will, it is hoped, proceed from an enlarged sample population.

Associated results. Several IMF-related properties of Pc 3,4 pulsations derived by earlier researchers have been automatically tested in this study. It has been asserted, for example, that Pc 4 occurrences are correlated with low field longitude, therefore with $\theta_{XB} \approx 0°$, but that Pc 3 occurrences are better correlated with the most common stream angle, i.e., field longitude $\approx 45°$ (Bol'shakova and Troitskaya, 1968). This result has received some theoretical support in a report by Kovner et al. (1976). The trend of Figure 3(b), however, is much the same,

though less pronounced, as that of 3(e), so the Pc 3 band appeared to share the same preference for low θ_{XB} as the Pc 4 band. The enhanced Pc 3 amplitudes of 3(c) between 20 and 40° could have been associated with the stream angle, but they seemed to form a separate group, and the Pc 4 data exhibited identical behavior for high K_p in 3(f). The present

data therefore do not support the differentiation of Pc 3 and 4 found by Bol´shakova and Troitskaya, and we are inclined to the tentative view that studies of this nature are very easily influenced by mixed phenomena.

A pair of related Soviet findings are that the period of micropulsations in the Pc 3-4 range are inversely related to both K_p (Jacobs, 1970, Figure 2.11) and interplanetary field magnitude B (Troitskaya et al., 1971). The K_p relationship contains a great deal of scatter, but on the average, yields divisions at $K_p = 2$ and 5; i.e., if $K_p \leq 2$, Pc 4 are stimulated, if $2 < K_p < 5$, Pc 3 appear, and if $K_p \geq 5$, the period of pulsations show no further K_p-dependence. Figure 3 does not support this relationship, for if it were correct, there would have been no Pc 3 signals when $K_p \leq 2$ [Figure 3(b)], and no trend above threshold should have been apparent. By the same reasoning, there should have been little or no evidence of Pc 4 activity when $K_p > 2$, as in 3(f), but the amplitudes were not only appreciable but showed the same underlying trend toward large signals near $\theta_{XB} = 0°$. We cannot deny the published K_p relationship which, although diffuse, was apparent. We believe rather that other factors, perhaps related in turn to K_p, were dominant.

One such factor, the field strength B, tends to be above average when K_p is elevated, and, as noted, gave a much sharper correlation with micropulsation period. In fact, the expression T(sec) = 160/B(γ) fits the data rather well (Gul´yel´mi et al., 1973). We have used this expression to isolate those hours when B should have determined that Pc 4 would be present, i.e., when $B \lesssim 3.5$, with the result shown in Figure 9. The by now familiar trend is evident, but there is still scatter, and the number of observations

has been so reduced as to make further discussion pointless at this stage. Moreover, a recent analysis by Russell and Fleming (1976) indicates that a correction of the B-relation may be needed. Since B's < 3.5γ were rare in the sample, most of the data should have involved the Pc 3 channel, and the analogous plot to Figure 9, not shown, was essentially similar to Figure 3(a). We note that the trend in Pc 4 behavior with θ_{XB} was apparent without Figure 9, and we doubt that taking B into account is essential to the relationship we are now investigating, although it may help to organize the data as the study progresses to larger samples.

The trend and the model. Subject to the qualifications already discussed regarding lack of Pc 3,4 distinction, the results appear to confirm as a general tendency the correlation of Pc events with low θ_{XB} demonstrated by others, as cited. We do prefer to emphasize the probability of signals above threshold rather than individual events, or actual amplitudes, at least until all the contributing factors are disentangled.

But what of the model? There is no conclusive direct proof here that the model of shock structural origin has been validated. On the other hand, there is no property of the data presented that is incompatible with the model, while two characteristics can be interpreted as highly encouraging. First, the unity of behavior of the signals whose periods disregard the Pc 3, 4 separation at T = 45 sec is what we would expect from a phenomenon dependent on the broad spectrum of noise in the magnetosheath (Siscoe et al., 1967; Fairfield and Ness, 1970) which has no such separation, but which does display distinguishable narrowband waves around the local, doppler-

shifted cyclotron frequency (see Fairfield and Behannon, 1976; Greenstadt et al., 1976). Remember that the ion cyclotron period follows a $T \propto B^{-1}$ dependence. Actually, for protons $T_c = (160/B)/2.44$; the factor 2.44 may represent an average correction of T_c for the magnetosheath rather than the solar wind, i.e., $T_c = 2.44\ (T_{cSW})$. Alternatively, the analysis by Kovner et al. (1976) gives the theoretical result $T = 2.5\ T_c$ for Doppler-shifted upstream waves in the solar wind itself, and these waves may find their way to the magnetopause directly.

Second, the apparent tendency for the probability of micropulsation noise enhancement to rise abruptly when $\theta_{XB} \lesssim 50\text{-}60°$ or, conversely, for the noise to be cut off sharply when $\theta_{XB} \gtrsim 60°$, is compatible with a property of the bow shock so specialized as to disparage coincidence. The angles $\theta_{XB} \lesssim 51°$ define just those orientations of $\underset{\sim}{B}$ for which the subsolar point of the bow shock is in the quasi-parallel regime if the value $p = 1.6$ is used to compute the angle of structural changeover (Greenstadt, 1974), and $p = 1.6$ is just the appropriate value to use at the subsolar point (Diodato et al., 1976). Indeed, the largest $\theta_{XB(MIN)}$ for which an amplitude significantly above threshold was recorded for both Pc 3 and Pc 4 under quiet conditions was 51° [Figures 3(b) and (e)].

Zero-degree enhancement. If the property discussed in the preceding paragraph is real, that is if micropulsations of tens of seconds period are excited at all angles for which quasi-parallel structure is established at the subsolar point of the bow shock, then the question arises of why the excitation should be radically enhanced when the field is aligned within about 5° of the X-axis. We do not have any physical explanation for this effect at present, but we can point out that geometrically 5° is about the angle at which the entire bow shock assumes quasi-parallel structure. This

condition is evidently extremely favorable to the transfer of waves to, and through, the magnetopause, if the shock is truly their source. However, it appears that disturbed magnetospheric conditions [Figures 3(c), (f)] may also favor enhanced excitation, perhaps for a different reason. Deeper understanding of these phenomena will require theoretical study as well as further data analysis.

Final remark. If further investigation substantiates the relationships described here, shock pulsation structure will provide a plausible source for the excitation of waves at the magnetosphere that are detected as Pc 3-4 micropulsations on the daylight side of the earth's surface. We think it not premature to express the hope that for at least one type of medium-period micropulsations we will soon be able to replace the heuristic designations Pc 3,4 and their arbitrary separation at T = 45 sec with a physically-based designation such as PCSO, "Continuous Pulsations of Shock Origin," spanning the minimal period range from 20 to 150 sec.

ACKNOWLEDGMENTS

The cooperation of the University of Calgary in providing space is gratefully acknowledged. This study was supported by National Aeronautics and Space Administration Contract NASW-2877 and the National Research Council of Canada. Continuing discussions with R. W. McPherron and C. Arthur and the diligent help of J. Burgess with data reduction have contributed strongly to this investigation.

REFERENCES

Arthur, C. W., R. L. McPherron, and P. J. Coleman, Jr., Micropulsations in the Morning Sector, 1, Ground Observations of 10- to 45-Second Waves, Tungsten, Northwest Territories, Canada, J. Geophys. Res., 78, 8180, 1973.

Bol´shakova, O. V., and V. A. Troitskaya, Relation of the Interplanetary Magnetic Field Direction to the System of Stable Oscillations, Dokl. Akad. Nauk., 180, 4, 1968.

Diodato, L., E. W. Greenstadt, G. Moreno, and V. Formisano, A Statistical Study of the Upstream Wave Boundary Outside the Earth's Bow Shock, J. Geophys. Res., 81, 199, 1976.

Fairfield, D. H., and K. W. Behannon, Bow Shock and Magnetosheath Waves at Mercury, J. Geophys. Res., in press, 1976.

Fairfield, D. H., and Ness, N. F., Magnetic-Field Fluctuations in the Earth's Magnetosheath, J. Geophys. Res., 75, 6050, 1970.

Fukunishi, H., and L. J. Lanzerotti, ULF Pulsation Evidence of the Plasma-Pause. 2. Polarization Studies of Pc 3 and Pc 4 Pulsations near L = 4 and at a Latitude Network in the Conjugate Region, J. Geophys. Res., 79, 4632, 1974.

Gokhberg, M. B., O. A. Pokhetelov, and Ye. B. Kocharyants, The Generation of Stable Oscillations in the Geomagnetic Field, Dokl. Akad. Nauk., 198, 8, 1971.

REFERENCES (Cont'd)

Greenstadt, E. W., Observation of Nonuniform Structure of the Earth's Bow Shock Correlated with Interplanetary Field Orientation, J. Geophys. Res., 77, 1729, 1972a.

Greenstadt, E. W., Field-Determined Oscillations in the Magnetosheath as Possible Source of Medium-Period, Daytime Micropulsations, Proc. of Conference on Solar Terrestrial Relations, University of Calgary, 515, April 1972b.

Greenstadt, E. W., Binary Index for Assessing Local Bow Shock Obliquity, J. Geophys. Res., 77, 5467, 1972c.

Greenstadt, E. W., Structure of the Terrestrial Bow Shock, Solar Wind Three, Proc. Third Solar Wind, Conf., Asilomar, ed C. T. Russell, Inst. Geophys. & Planet. Phys., UCLA, 440, 1974.

Greenstadt, E. W., I. M. Green, G. T. Inouye, D. S. Colburn, J. H. Binsack, and E. F. Lyon, Dual Satellite Observation of the Earth's Bow Shock. 3. Field-Determined Shock Structure, Cosmic Electrodyn., 1, 316, 1970.

Greenstadt, E. W., C. T. Russell, V. Formisano, P. C. Hedgecock, F. L. Scarf, M. Neugebauer, and R. E. Holzer, Structure of the Quasi-Parallel, Quasi-Laminar Bow Shock, submitted to J. Geophys. Res., 1976.

Gul'yel'mi, A. V., T. A. Plyasova-Bakunina, and R. V. Schepetnov, Relation Between the Period of Geomagnetic Pulsations Pc 3,4 and the Parameters of the Interplanetary Medium at the Earth's Orbit, Geomag. & Aeron., 13, 331, 1973.

Jacobs, J. A., Geomagnetic Micropulsations, Springer-Verlag, New York, 1970.

REFERENCES (Cont'd)

Kovner, M. S., V. V. Lebedev, T. A. Plyasova-Bakunina, and V. A. Troitskaya, On the Generation of Low-Frequency Waves in theSolar Wind in the Front of the Bow Shock, Planet. Space Sci., 24, 261, 1976.

Mihalov, J. D., D. S. Colburn, R. G. Currie, and C. P. Sonett, Configuration and Reconnection of the Geomagnetic Tail, J. Geophys. Res., 73, 943, 1968.

Nourry, G., and T. Watanabe, Geomagnetic Pulsations and Solar Wind, Abstract, Second General Scientific Assembly, Kyoto, IAGA Bulletin No. 34, 395, 1973.

Plyasova-Bakunina, T. A., Effect of the Interplanetary Magnetic Field on the Characteristics of Pc 3-4 Pulsations, Geomag. and Aeron., 12, 675, 1972.

Russell, C. T., and B. K. Fleming, Remote Sensing of the Interplanetary Magnetic Field: Test of a Russian Index, submitted to Science, 1976.

Samson, J. C., J. A. Jacobs, and G. Rostoker, Latitude-Dependent Characteristics of Long-Period Micropulsations, J. Geophys. Res., 76, 3675, 1971.

Santirocco, R. A., and D. G. Parker, The Polarization and Power Spectrums of Pc Micropulsations in Bermuda, J. Geophys. Res., 68, 5545, 1963.

Siscoe, G. L., L. Davis, Jr., E. J. Smith, P. J. Coleman, Jr., and D. E. Jones, Magnetic Fluctuations in the Magnetosheath: Mariner 4, J. Geophys. Res., 72, 1, 1967.

Troitskaya, V. A., T. A. Plyasova-Bakunina, and A. V. Gul'yel'mi, Relationship Between Pc 2-4 Pulsations and the Interplanetary Magnetic Field, Dokl. Akad. Nauk., 197, 1312, 1971.

Wolfe, A., and R. L. Kaufmann, MHD Wave Transmission and Production near the Magnetopause, J. Geophys. Res., 80, 1764, 1975.

FIGURE CAPTIONS

Figure 1. Comparison of θ_{XB} and Pc 4 X-axis waveforms for (a) a day of consistently high θ_{XB} and (b) a day of consistently low θ_{XB}.

Figure 2. Comparison of θ_{XB} and Pc 3 and Pc 4 waveforms for six hours centered on local noon on six days representing various degrees of correlation. Dates and selected magnetometer axes are indicated at the bottoms of the respective panels.

Figure 3. Scatter plots of hourly Pc 3 and Pc 4 peak-to-peak amplitudes vs hourly minimal θ_{XB}. Left, all data; center, undisturbed hours; right, disturbed hours. Maxima and minima in each 5° range marked by histograms.

Figure 4. Positions of the moon, around which Explorer 35 orbits, relative to the magnetosphere in the solar ecliptic XY plane during the interval for which spectral data were examined. Numbers along the outside of the Explorer 35 circle denote 0000 UT of the corresponding dates, from 2 to 20 September 1969. The diagonal lines mark the dates and positions of Explorer 35 at the approximate extremes of nominal corotation delay times from the spacecraft to the earth. The marked delays are for spacecraft time minus earth time. The +19 min notation signifies a maximal, nominal convection delay that could have applied on 12 September. All distances are in earth radii (R_E).

Figure 5. High resolution comparison of θ_{XB} and Pc 4 activity surrounding local noon on days of approximately zero nominal corotation delay. (a) 7 September, (b) 8 September 1969.

FIGURE CAPTIONS (Cont'd)

Figure 6. Comparison of θ_{XB} (upper panels) and Pc 3-4 power spectral density (lower panels) for the same two days of consistently high θ_{XB} (a) and low θ_{XB} (b) as in Figure 1. Power level is computed for 32-minute segments with 50 percent overlap and is indicated by the symbols defined in Figure (a).

Figure 7. Comparison of θ_{XB} and Pc 3-4 power spectral density during a pre-noon interval when θ_{XB} shifted from low to high levels. Symbols have the same meanings as in Figure 6.

Figure 8. Comparison of θ_{XB} and Pc 3-4 power spectral density for two days in which the waveform correlation was shown to have been poor.
(a) 7 September, high-resolution waveform in Figure 5(a);
(b) 17 September, compressed timescale waveform in Figure 2(d).

Figure 9. Scatter plot of Pc 4 band hourly amplitude vs $\theta_{XB(MIN)}$ for those hours in which micropulsation activity should have been in the Pc 4 channel according to the Soviet formula $T = 160/B$.

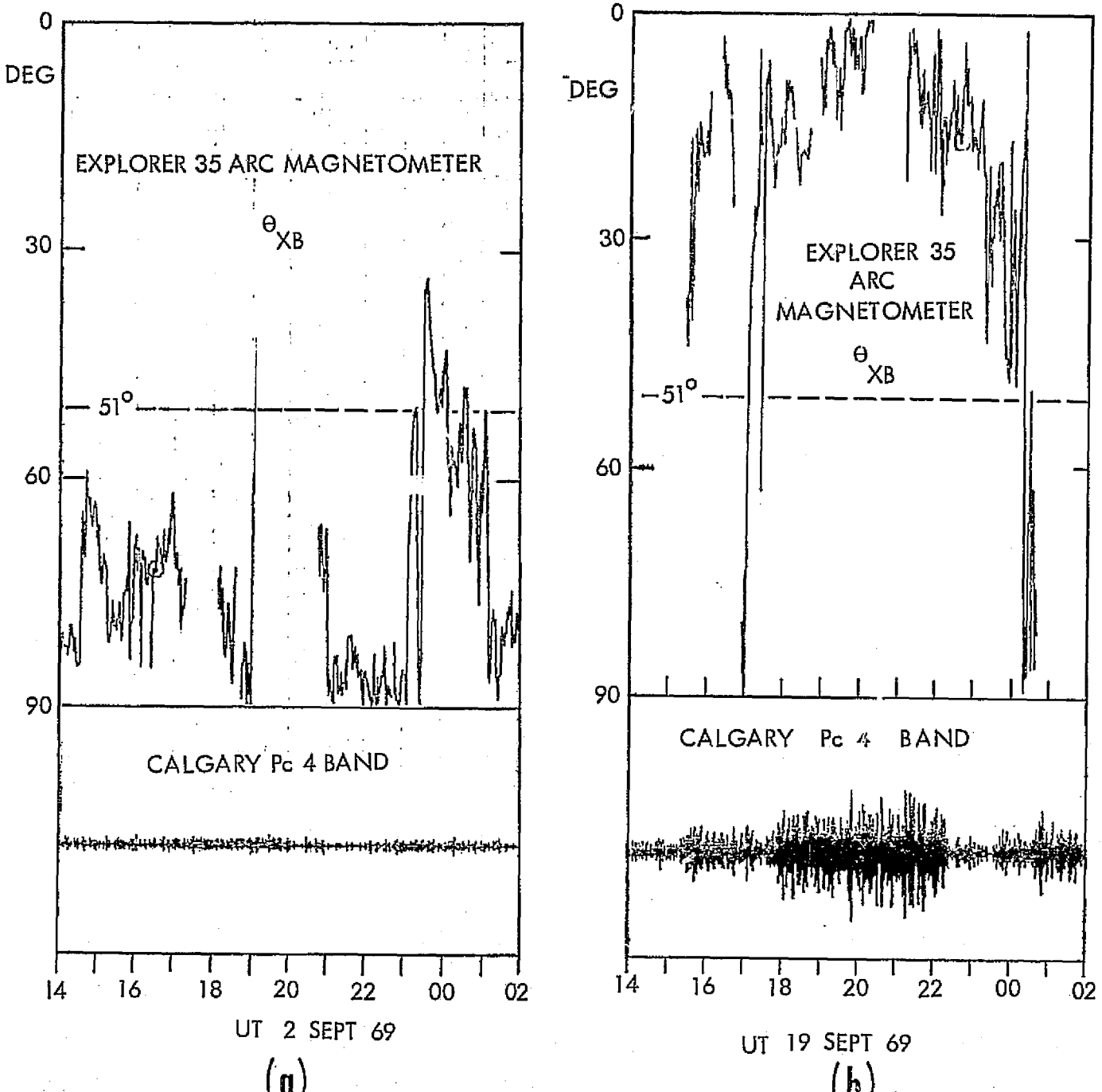

Figure 1. Comparison of θ_{XB} and Pc 4 X-axis waveforms for:
(a) A day of consistently high θ_{XB}
(b) A day of consistently low θ_{XB}

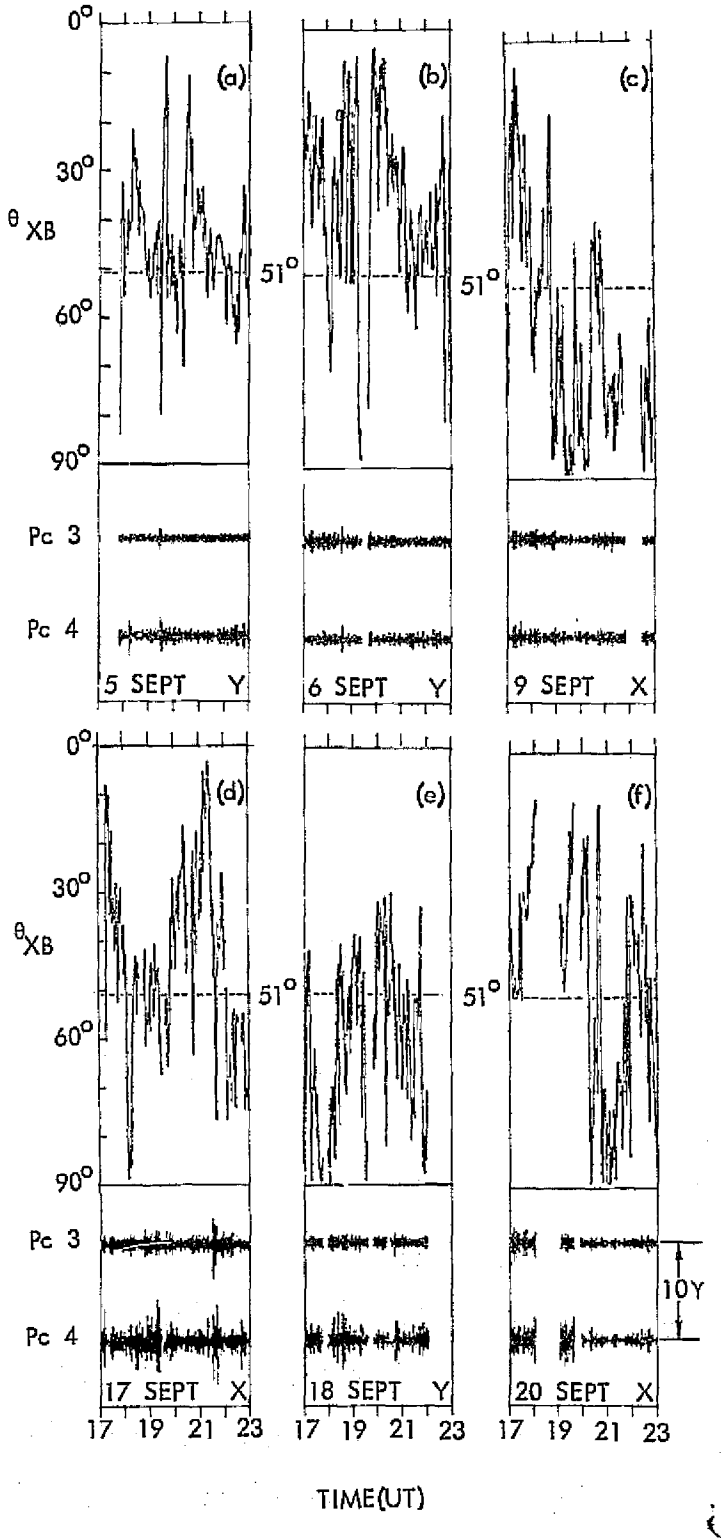

Figure 2. Comparison of θ_{XB} and Pc 3 and Pc 4 waveforms for six hours centered on local noon on six days representing various degrees of correlation. Dates and selected magnetometer axes are indicated at the bottoms of the respective panels.

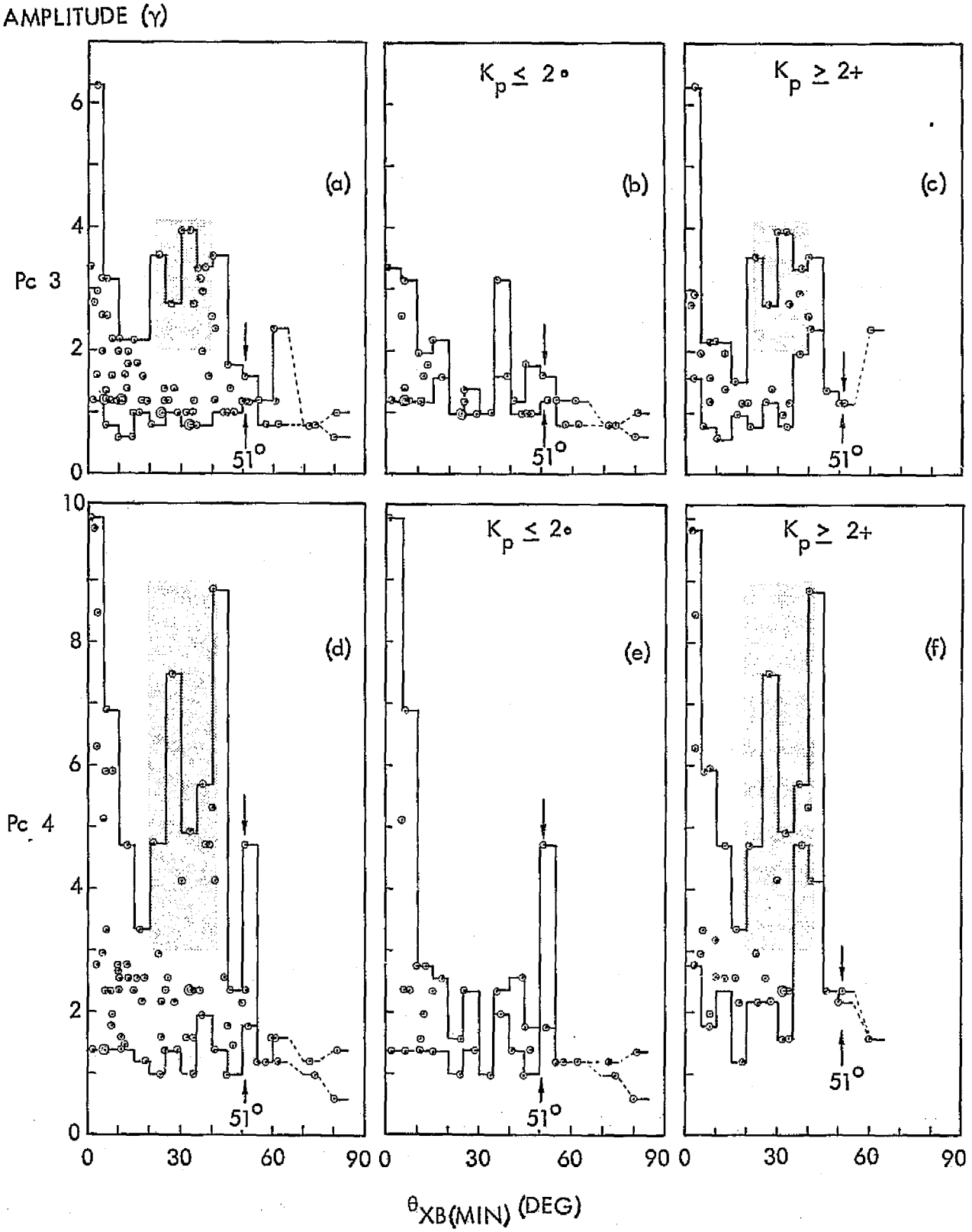

Figure 3. Scatter plots of hourly Pc 3 and Pc 4 peak-to-peak amplitudes vs hourly minimal θ_{XB}. Left, all data; center, undisturbed hours; right, disturbed hours. Maxima and minima in each 5° range marked by histograms.

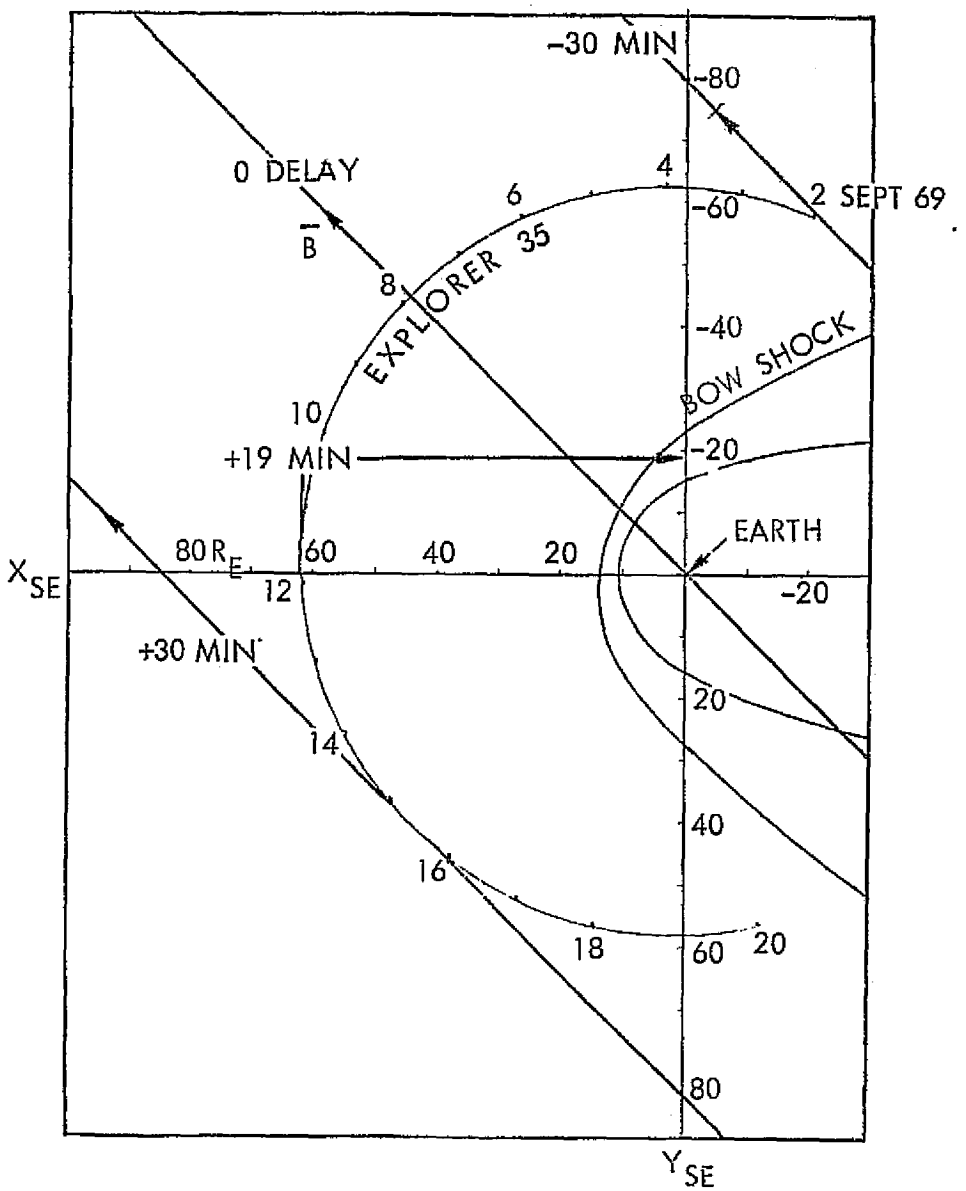

Figure 4. Positions of the moon, around which Explorer 35 orbits, relative to the magnetosphere in the solar ecliptic XY plane during the interval for which spectral data were examined. Numbers along the outside of the Explorer 35 circle denote 0000 UT of the corresponding dates, from 2 to 20 September 1969. The diagonal lines mark the dates and positions of Explorer 35 at the approximate extremes of nominal corotation delay times from the spacecraft to the earth. The marked delays are for spacecraft time minus earth time. The +19 min notation signifies a maximal, nominal convection delay that could have applied on 12 September. All distances are in earth radii (R_E).

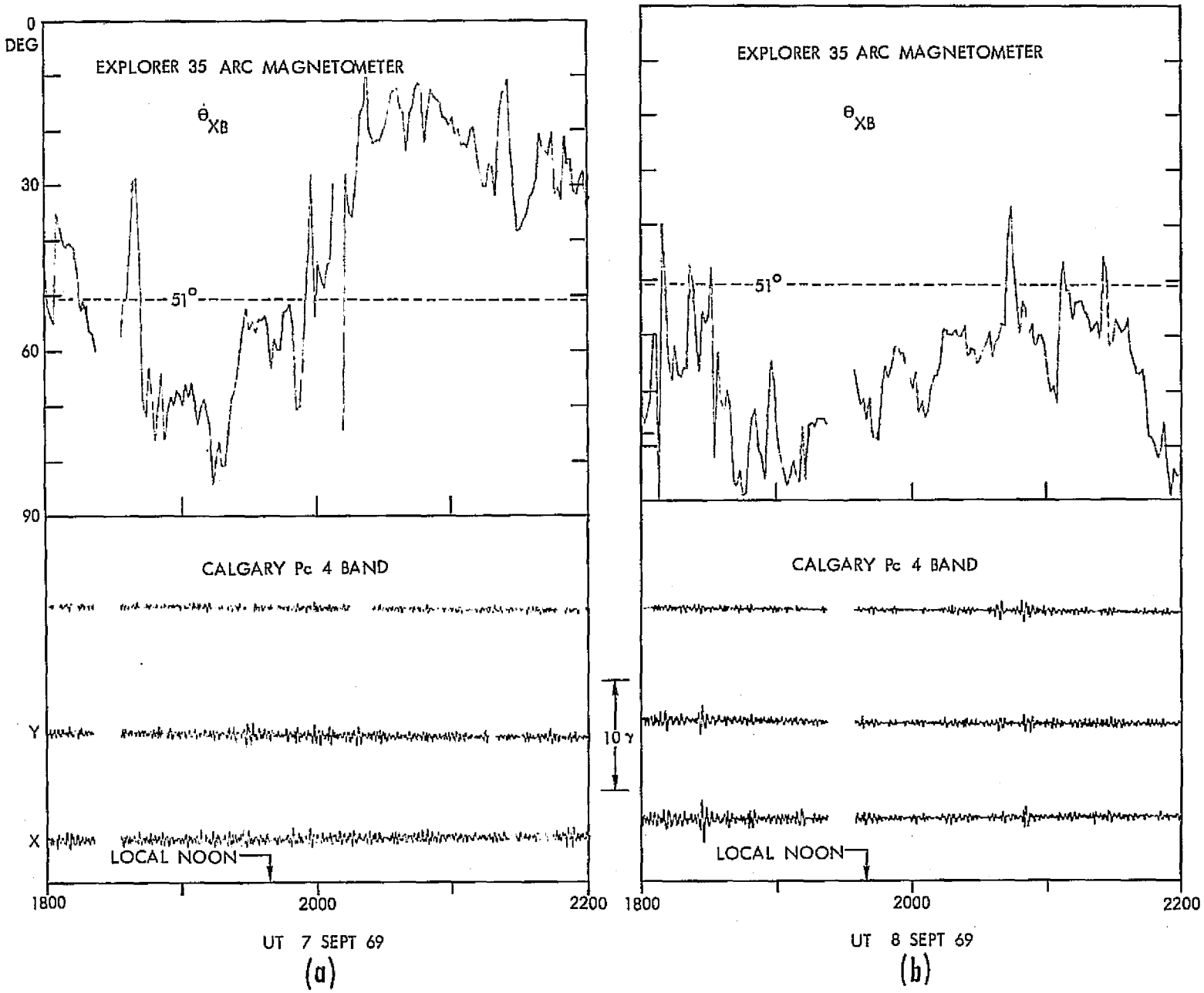

Figure 5. High resolution comparison of θ_{XB} and Pc 4 activity surrounding local noon on days of approximately zero nominal corotation delay. (a) 7 September, (b) 8 September 1969.

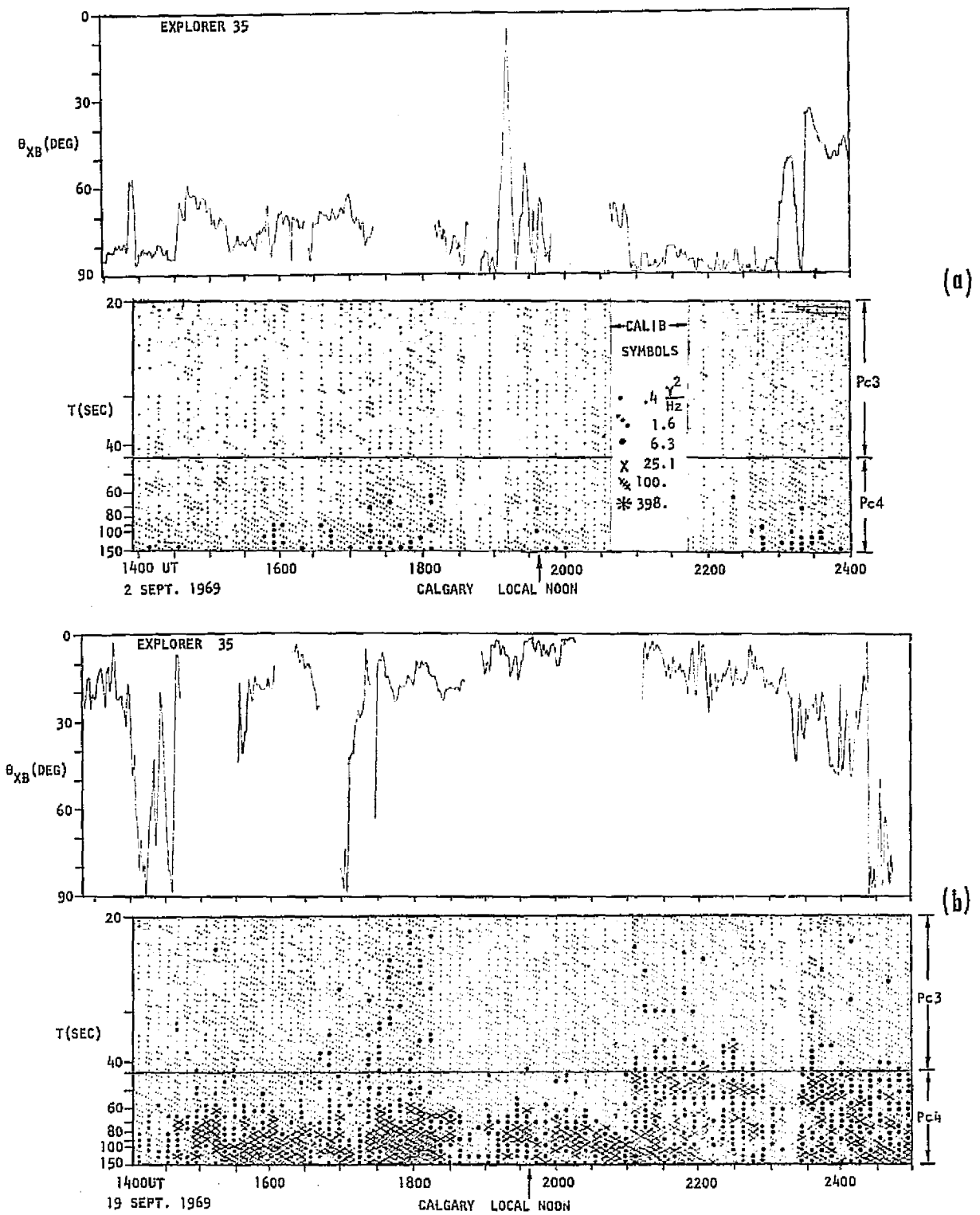

Figure 6. Comparison of θ_{XB} (upper panels) and Pc 3-4 power spectral density (lower panels) for the same two days of consistently high θ_{XB} (a) and low θ_{XB} (b) as in Figure 1. Power level is computed for 32-minute segments with 50 percent overlap and is indicated by the symbols defined in Figure (a).

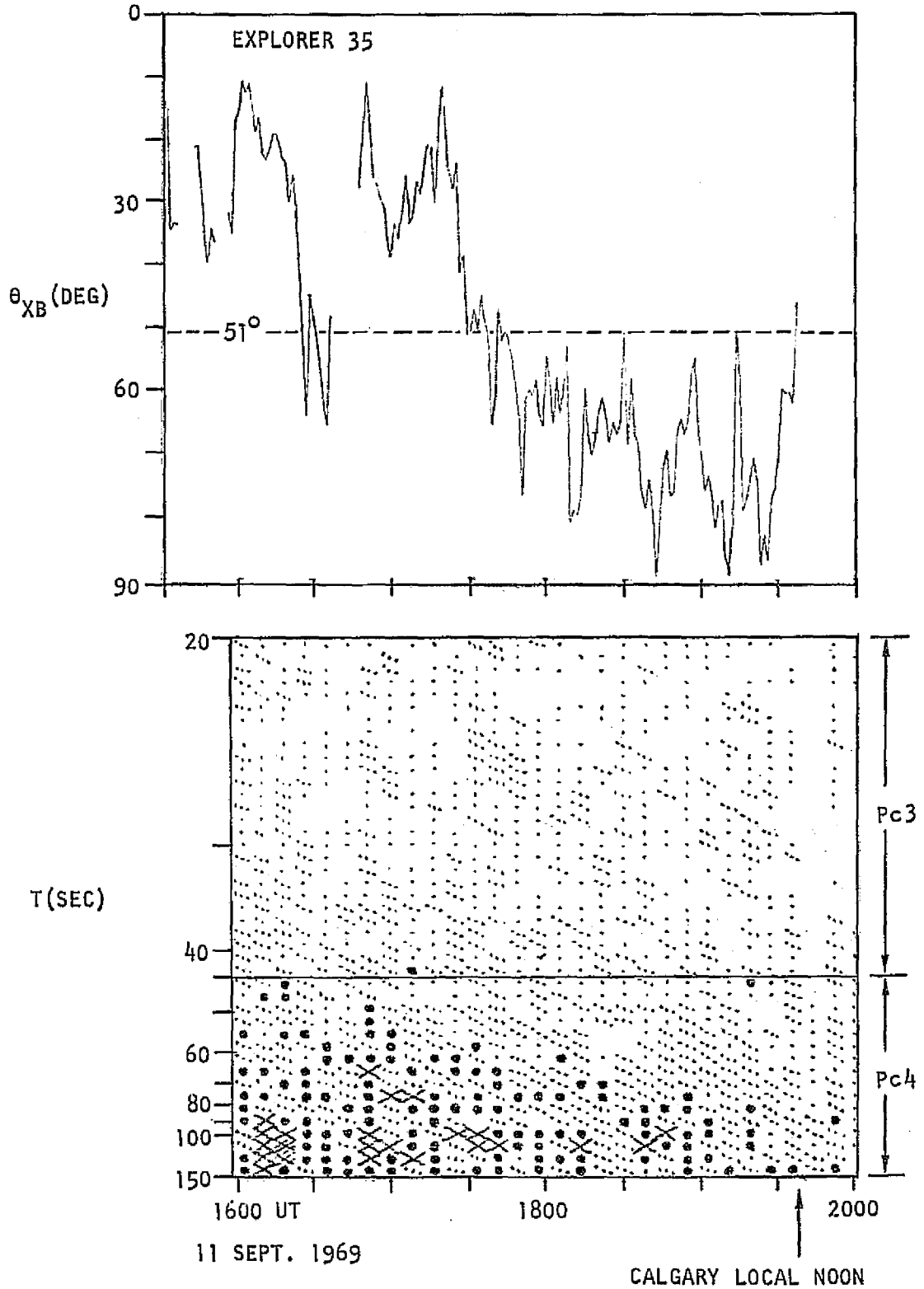

Figure 7. Comparison of θ_{XB} and Pc 3-4 power spectral density during a pre-noon interval when θ_{XB} shifted from low to high levels. Symbols have the same meanings as in Figure 6.

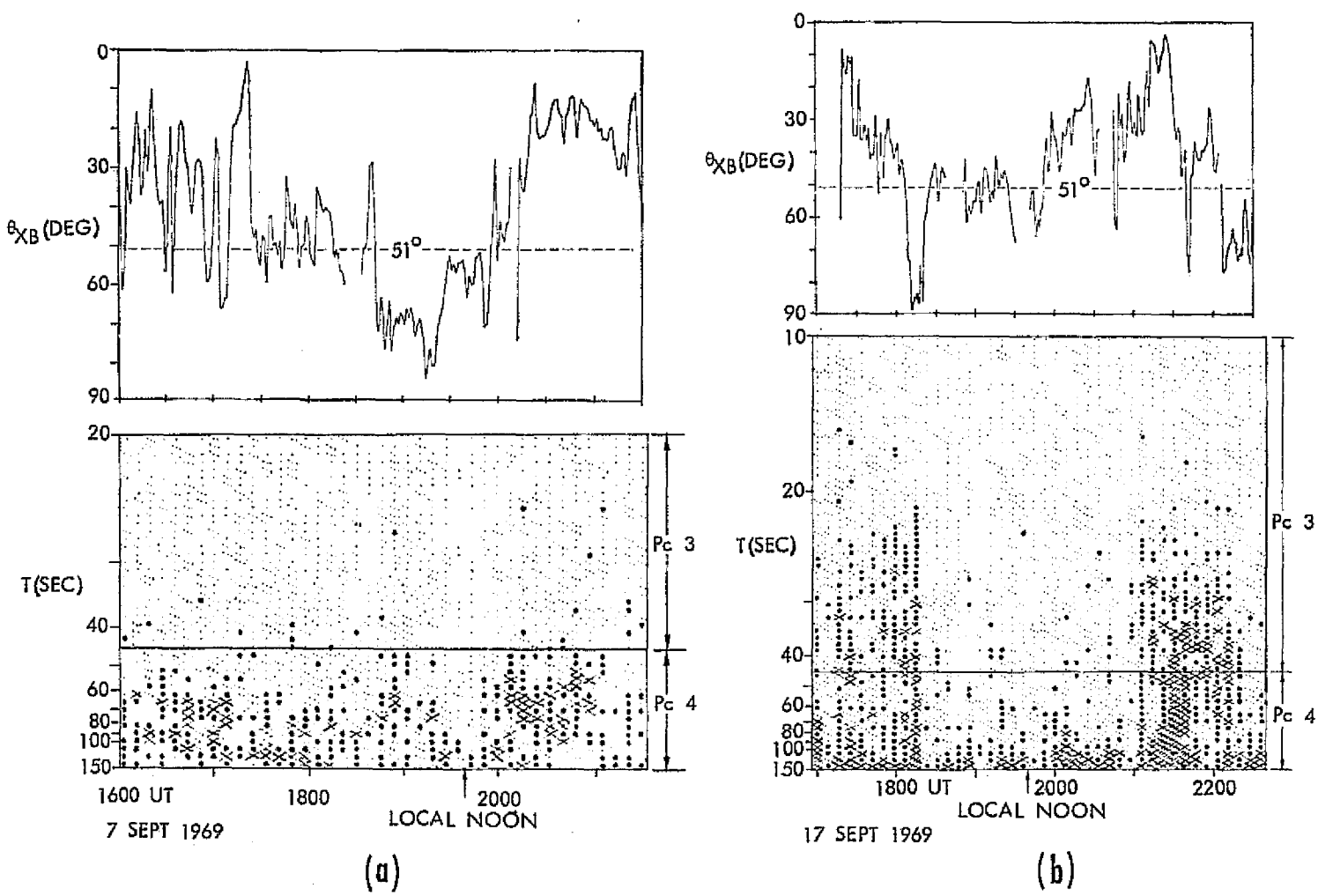

Figure 8. Comparison of θ_{XB} and Pc 3-4 power spectral density for two days in which the waveform correlation was shown to have been poor.
(a) 7 September, high-resolution waveform in Figure 5(a);
(b) 17 September, compressed timescale waveform in Figure 2(d).

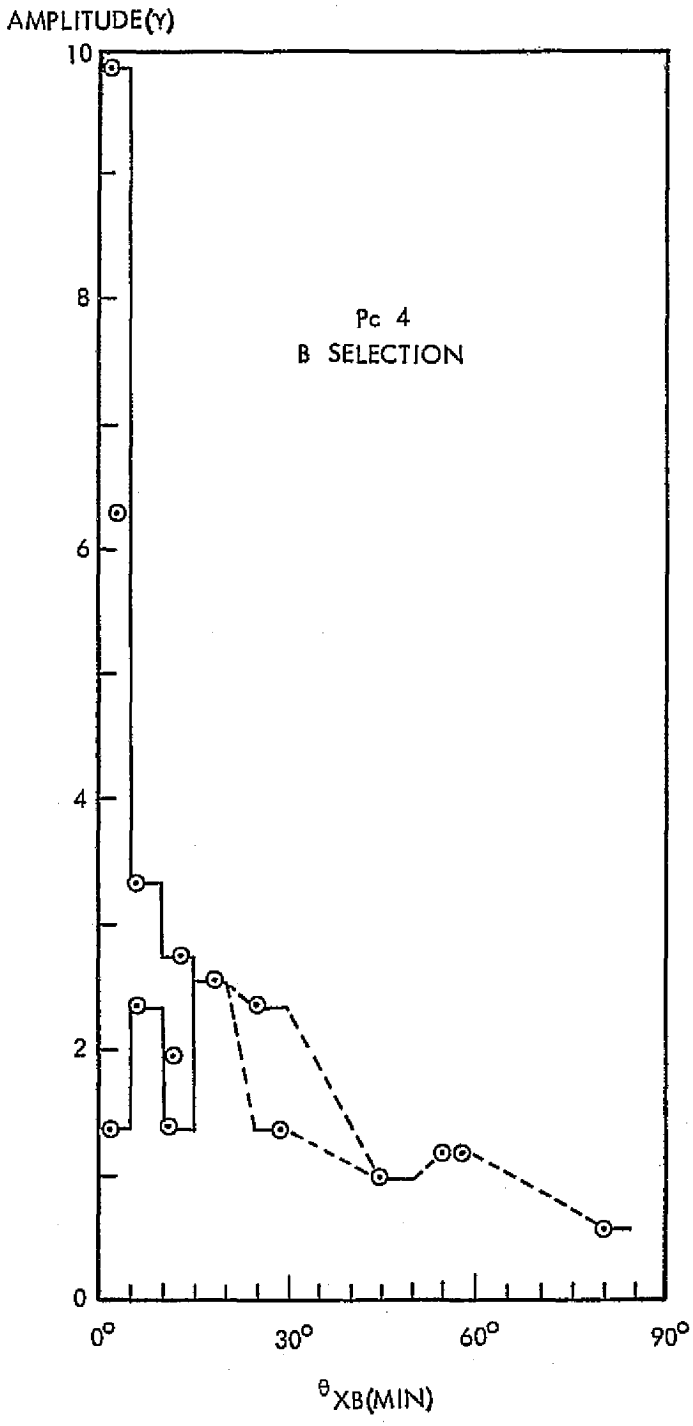

Figure 9. Scatter plot of Pc 4 band hourly amplitude vs $\theta_{XB(MIN)}$ for those hours in which micropulsation activity should have been in the Pc 4 channel according to the Soviet formula T = 160/B.

APPENDIX 2

CONTRIBUTION TO A REPORT: "THE THIN BOW SHOCKS OF 24 MARCH 1969"

This document is part of a contribution to the follow-on to an initial draft manuscript entitled "Possible Identification of a Perpendicular Bow Shock." The authors are V. Formisano, C. T. Russell, J. Means, E. W. Greenstadt, F. L. Scarf, and M. Neugebauer.

APPENDIX 2

THE THIN BOW SHOCKS OF 24 MARCH 69

Five shocks were observed which were thin by crude visual standards, for they all displayed their principal magnetic ramps in less than a dozen, and as few as one or two points at OGO's eight kilobit rate, i.e., in .14 to 1.7 seconds at .144 seconds/sample. Since the several crossings occurred in a half-hour interval, the bow shock was certainly not stationary, but if we choose what we may call the "traditional nominal" shock velocity of 10 km/sec, often used when no better information is available, we obtain ramp thicknesses L_s between 1.4 and 17 km. The shortest applicable value of c/ω_{pi} based on solar wind data during the observation interval was about 40 km, so the thickest observed ramp would have been less than half this customary unit of measure for quasi-perpendicular, oblique shocks. More persuasive still, is the argument that a high shock velocity (relative to the spacecraft) of 200 km/sec applied to the shortest recorded ramp time of .144 sec would give L_s = 29 km, still less than the shortest estimated c/ω_{pi}. Superficially, then, at least some of the bow shocks of 24 March appear to have been "thin" in the sense that $L_s < c/\omega_{pi}$, the expected measure of oblique shocks.

It has recently been proposed that a marginal stability criterion for ion acoustic waves can be applied to the bow shock to provide values of L_s independent of c/ω_{pi} (Morse and Greenstadt, 1976). Values $L_s < c/\omega_{pi}$ would occur in a straightforward way in a suitable upstream combination of N, ΔB, and T_e/T_i. While the adopted theory had been developed strictly for perpendicular shocks, it seemed to work well for several thick, laminar shock observations even when θ_{nB} was as little as 60°. The same criterion can be

applied here in an attempt to arrive at some estimates of L_s, because the angle $\theta_{nB} \approx 70°$ is reasonably favorable to the perpendicular approximation and the magnetic ramps are strongly indicative of a single dominant current layers.

A convenient summary version, in hybrid units, of the formula used is:

$$L_s(\text{km}) = 1.9 \frac{\Delta B_x(\gamma)}{N(\text{cm}^{-3}) f(T_e/T_i)} \quad , \tag{1}$$

where ΔB_x is the difference between the ramp-top and ramp-bottom field component in the shock plane, and function $f(T_e/T_i)$ is obtained from a numerically computed curve of marginal ion acoustic stability (Fried and Gould, 1961). The appropriate curve segment and the original expression in mks units will be found in the paper of Morse and Greenstadt (1976). For comparison, a set of "observed" thicknesses was estimated from a strictly empirical model of the shock's motion that could have produced the observed pattern of crossings in half an hour.

The thicknesses L_s calculated for the first shocks are plotted in the accompanying figure superposed on Figure 3 from the paper of Morse and Greenstadt (1976). The straight line represents the condition that the calculated and observed shock thicknesses agree, and the five unlabeled data flags show the results of the earlier study. Both the ranges (shaded) and the midvalues (flags) are presented in the figure.

If the tentative results in the figure are not radically revised, stable ion acoustic wave generation in the shock ramp will lead to estimates of "short" thicknesses that are compatible with whatever simple tests we are able to make of them, including a comparison with observed thicknesses derived from a first order model of the shock's motion during the data interval.

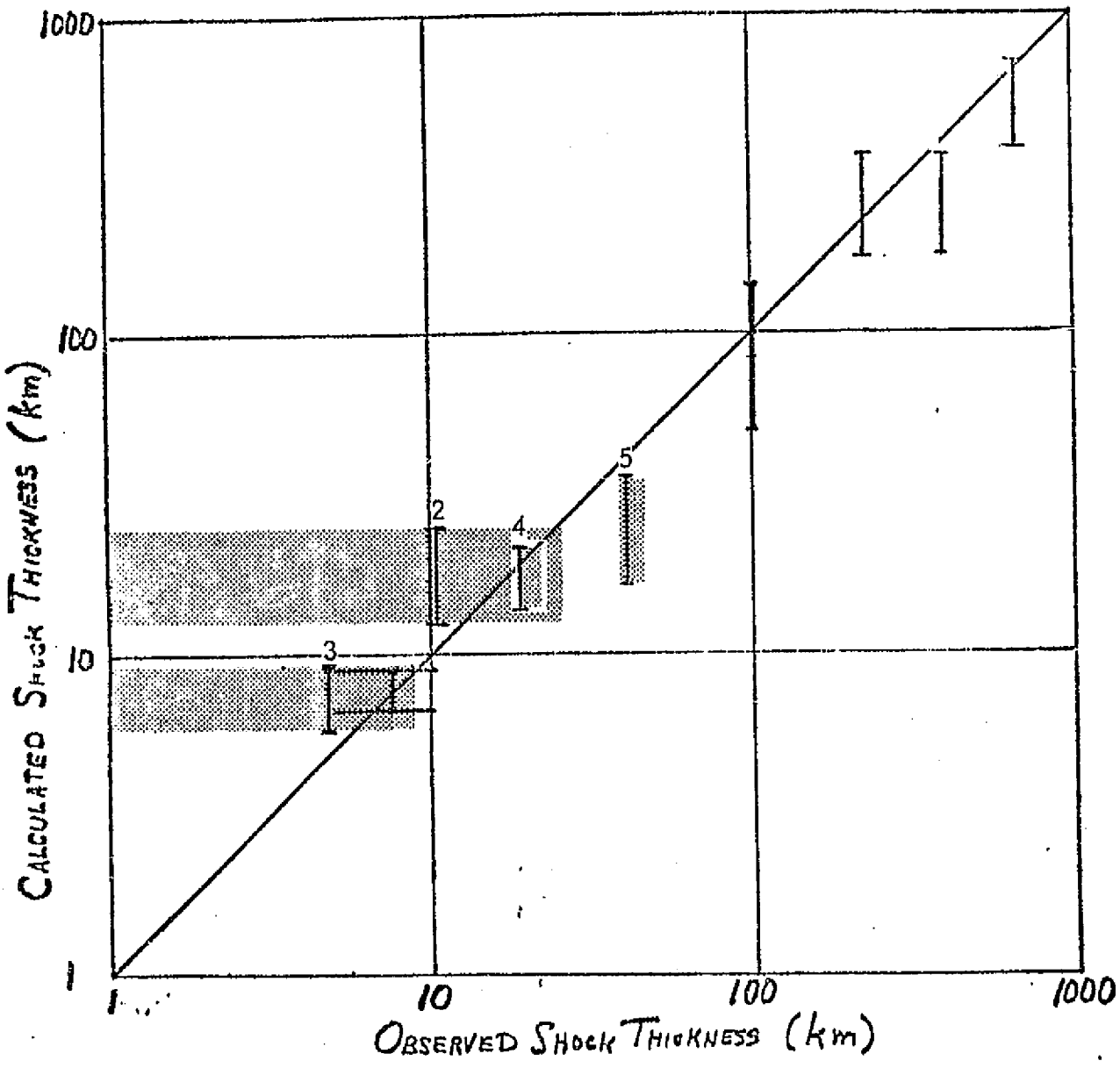
1000
100
10
1
1
10
100
1000
Calculated Shock Thickness (km)
Observed Shock Thickness (km)
2
3
4
5

APPENDIX 3

Vol. 3, No. 9 Geophysical Research Letters September 1976

ENERGIES OF BACKSTREAMING PROTONS IN THE FORESHOCK

E. W. Greenstadt

Space Sciences Department, TRW Defense & Space Systems Group
One Space Park, Redondo Beach, California 90278

Abstract. A predicted pattern of energy vs detector location in the cislunar region is displayed for proton guiding-centers traveling upstream away from the quasi-parallel bow shock. The pattern is implied by upstream wave boundary properties deduced by Diodato et al. (1976). In the solar ecliptic, protons are estimated to have a minimum of 1.1 times the solar wind bulk energy E_{SW} when the wave boundary is in the early morning sector and a maximum of 8.2 E_{SW} when the boundary is near the predawn flank.

Introduction

At least some part of the cislunar solar wind region outside the earth's bow shock is continuously populated by particles and waves of shock or magnetospheric origin. The varying precursor region, or foreshock, is divided into several subregions, not all geometrically distinct, which are defined by differing particle species and wavemodes. One such subregion is characterized by the presence of backstreaming (hereinafter called "return") protons of energy a few times the solar wind bulk flow energy and long-period, say 10 to 60-second, magnetic waves of amplitude about one-quarter of the magnitude of the upstream field $\underset{\sim}{B}_{SW}$. The return protons are thought to produce the waves [Fairfield, 1969; Greenstadt et al., 1970; Barnes, 1970; Fredricks, 1975].

A correlation between the occurrence of beams of return protons of specific energy and the appearance of long period upstream waves has not yet been established experimentally by direct observation of both phenomena simultaneously. Nor is such a correlation likely in the immediate future. Statistical study of return particle properties does seem quickly attainable, however, and one test of both of the particle-wave relationship and of a recent result of Diodato et al. (1976) relating a wave boundary parameter to the location of the particle source at the shock would be to collect observations of return proton energies throughout the upstream region for many foreshock configurations. This note presents a first-order examination of the way in which the geometry of the foreshock wave boundary of Diodato et al. can be translated into a geometry of return proton energies.

Idealized Example

Detection Geometry. A beam of reflected bulk-velocity protons spirals away from the shock with guiding-center velocity components $V_{\|}$ parallel to $\underset{\sim}{B}_{SW}$ and drift V_d perpendicular to $\underset{\sim}{B}_{SW}$ according to the solution of $dV/dt = (\Omega_c/B_{SW})(-\underset{\sim}{V}_{SW}\times\underset{\sim}{B}_{SW}\times$ $\underset{\sim}{V}\times\underset{\sim}{B}_{SW})$ where Ω_c is the proton cyclotron frequency [Spitzer, 1962; Alfvén and Fälthammer, 1963; Benson et al., 1975]. A detector suitably oriented to accept the spiraling beam at its proper pitch angle in relation to the guiding center path will then see particles at some resulting energy E_r corresponding to net resultant velocity V_r.

In this report, only the simplest case of gyrationless particles is considered, so V_r and E_r represent just the guiding center resultant. The possibility that gyrationless particles cannot produce waves and are therefore unrelated to those that do produce the foreshock boundary is recognized, but we pass over this delicacy for the moment on the assumption that groups of return protons leave the shock together with a variety of pitch angles and we merely look selectively along the guiding-center path.

It has become customary to treat foreshock particles and waves as if the resultant guiding center velocity in the shock frame, in the plane of $\underset{\sim}{B}_{SW}$ and $\underset{\sim}{V}_{SW}$, were the vector sum of $\underset{\sim}{V}_{SW}$ and an apparent velocity along $\underset{\sim}{B}_{SW}$ [Asbridge et al., 1968; Fairfield, 1969], as shown in Figure 1. From this viewpoint, the speed along $\underset{\sim}{B}_{SW}$ is written as a multiple pV_{SW} of the solar wind speed, and the upstream, or sunward, boundary of the "proton-wave" foreshock is apparently well determined within contemporary experimental accuracy by a line tangent to the nominal bow shock cross section in the plane of X and $\underset{\sim}{B}_{SW}$ and at an angle to the solar ecliptic (SE) X-axis of θ_{XF} = arctan $[p \sin\theta_{XB}/(p\cos\theta_{XB}-1)]$ [Greenstadt, 1974; Diodato et al., 1976]. In this expression, θ_{XB}

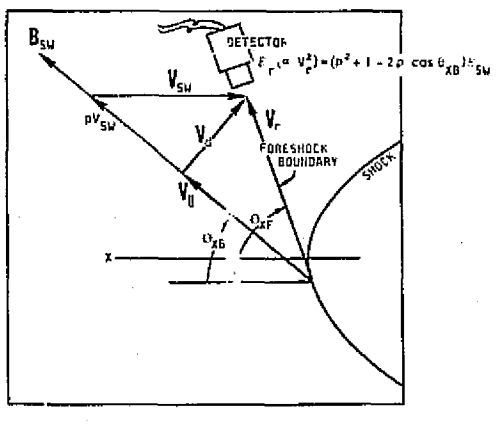

Fig. 1. Geometry of return proton detection. Particle guiding-centers in the plane of $\underset{\sim}{V}_{SW}$ (i.e., X) and $\underset{\sim}{B}_{SW}$ advance along $\underset{\sim}{B}_{SW}$ at speed $V_{\|}$ while drifting perpendicular to $\underset{\sim}{B}_{SW}$ at speed V_d, but resulting velocity $\underset{\sim}{V}_r$ is treated as if $\underset{\sim}{V}_r = pV_{SW}\underset{\sim}{B}_{SW}/B_{SW} + \underset{\sim}{V}_{SW}$.

is the angle between X and $\underset{\sim}{B}_{SW}$, and X and $\underset{\sim}{V}_{SW}$ have been taken to be colinear. Investigation has shown that p averages about 2.0 overall for the daylight portion of the shock, but appears from rough statistics to vary with the location of the tangent point, being about 1.6 in the subsolar region and rising above 2.0 toward the dawn and dusk flanks [Diodato et al., op cit]. In the estimates which follow, $\underset{\sim}{B}_{SW}$ has been assumed in the ecliptic.

First-Order Pattern. In Figure 2 the five segments of the dayside bow shock corresponding to the finest division described by Diodato et al. are shown symmetrically with respect to the solar ecliptic (SE) X-axis in an ecliptic-plane cross section. Connected to the nominal shock at each segment is an arc into which return protons would radiate outward from the shock with the apparent velocity component pV_{SW} along $\underset{\sim}{B}_{SW}$ for the depicted range of $\underset{\sim}{B}_{SW}$ directions. Protons are indicated in terms of their zero-pitch angle (gyrationless) energy as it would appear to a detector stationary in the earth frame and pointing into the direction from which the net return proton flux comes. The energy E_r is proportional to V_r^2, so from Figure 1, $E_r = (p^2 + 1 - 2p \cos\theta_{XB})E_{SW}$. The range of E_r's noted below p at the top of each arc section in Figure 2 corresponds to the range of angles θ_{XB} (inserts) that yield foreshock boundaries of angle θ_{XF} tangent to the shock within the sector.

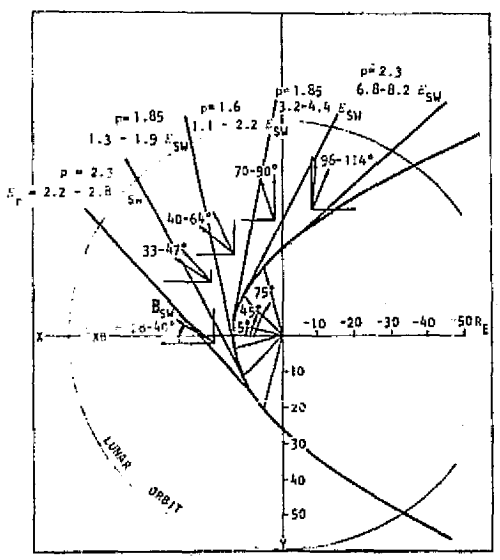

Fig. 2. Pattern of return particle guiding-center energy ranges for protons at the leading edge of the foreshock in five shock sectors determined by orientation of $\underset{\sim}{B}_{SW}$ in the ecliptic

What the picture tells us is that for $\underset{\sim}{B}_{SW}$ in the indicated direction ranges θ_{XB}, the foreshock wave boundary will lie in the corresponding sector radiating from the corresponding shock segment. Associated with the wave boundary in a given sector will be return protons of velocity $V_{\|}$ (or V_r) and energy E_r appropriate to the same segment. plane. The directions of $\underset{\sim}{B}_{SW}$ (arrows) and ranges of θ_{XB} which place the foreshock boundary in the various sectors are shown in the small insert frames. The pairs of numbers at the top of each sector give the average p over the sector (upper number) and the corresponding range of return energy E_r (lower number).

Discussion

The actual pattern of return particles will be somewhat different from the idealized one above, because foreshock boundary-protons will be neither unidirectional nor monoenergetic. There are four contributors to the spread in energies to be expected of ions coming from each segment. First, there ought to be the real pitch angle distribution of protons, and of course not all solar wind protons arrive at the shock with precisely the bulk velocity V_{SW} because of their thermal distribution.

Second, there may be a spectrum of p's associated with a given point of the shock even though only the ones found by Diodato et al. generate the waves.

Third, there is presumably a continuum of changing p values around the shock in three dimensions rather than averages over discrete zones in one plane as depicted. Time-changes in the non-ecliptic Z-component of $\underset{\sim}{B}_{SW}$ and in the solar wind velocity direction, which aberrates the shock axis of symmetry, would tend to produce a mixture of particle energies in any given backstream direction over almost any finite time interval. Also, there is no reason developed yet that compels the dominant p to be rigidly constant in time at a given point of the shock; local shock properties may affect the instantaneous value of p at any point.

Fourth, it seems likely that while the return protons coming from around the tangent point of the wave boundary at the shock have energies determined by the average p-relationship, protons coming from behind the foreshock boundary elsewhere on the quasi-parallel portion of the shock may be released upstream with higher guiding center velocities, thus intersecting the boundary at varying distances from the shock. A hypothetical intersection of return particles from three points of the shock is illustrated in Figure 3. With the field at angle θ_{XB} so that the foreshock wave boundary is determined by p = 1.6 near the subsolar point, the figure postulates a property of the quasi-parallel shock in which p rises with decreasing θ_{nB} to a sharp maximum when $\theta_{nB} = 0$ (corresponding to parallel shock structure), focusing beams of particle guiding centers on cislunar observation point O. The actual dependence of return particle energies on position of release along the shock or, more precisely, on θ_{nB}, for a given θ_{XB}, is still unmeasured, but it is known that 30 to 100 keV protons reach the moon's distance at about the same position as does the average foreshock boundary for $\theta_{XB} \approx 45°$ [Lin et al., 1974]. The dashed lines continuing outward from O in Figure 3 call attention to the possibly complex pattern of the position-dependent particle population that may form the upstream signature for a given θ_{XB}.

For any θ_{XB}, protons coming from the shock

along the foreshock boundary and responsible for the long-period foreshock waves should be distinguishable from most others by their average direction of arrival. The important information in Figure 2 therefore is the trend in foreshock proton guiding-center energies that can be expected for different positions of the wave boundary, from the viewpoint of a suitably-oriented detector. The anticipated trend includes a dip to minimal energies in the early to midmorning region of the foreshock and rather high energies near the western flank. The dip corresponds to the most probable interplanetary field orientations; the higher energies at the flank should be relatively unusual, since the responsible field directions are uncommon.

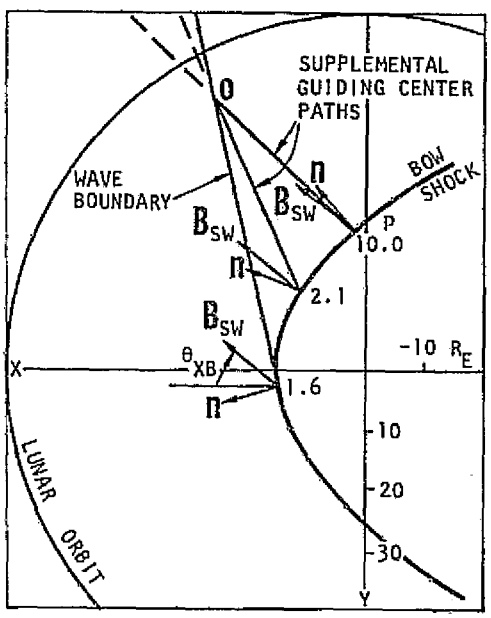

Fig. 3. Hypothetical example of a possible cislunar convergence of return protons of mixed energies. For a fixed B_{SW} (in the ecliptic) the local value of p, indicated at three locations along the inside of the shock, could increase dramatically with the local approach to parallel structure, i.e., B_{SW} parallel to the local normal n. Fast protons with p = 10 could arrive from the flank at the same observation point Q as slower protons with p = 1.6 arrive from the subsolar region.

We may hope eventually to interpret an observed E_r in terms of the corresponding proton beam's original characteristics. However, no V_r is produced uniquely by a single combination of parallel and perpendicular return particle velocities, so there is an intrinsic ambiguity in relating measurements of E_r to the energy and angle distribution of particles emitted at the shock. A full characterization of foreshock particle and wave properties, including interactions with the incoming solar wind will therefore be a complicated undertaking. Until at least an initial experimental survey is completed, it appears unpromising to attempt a full-scale description of all the observational results that could be inferred from a continuum of assumed pitch angles and production parameters. An appreciation of some complexities associated with the latter can be obtained from an elementary study of the proton escape problem [Greenstadt, 1975].

Conclusion

There is an idealized pattern of directions and energies of return proton guiding-centers traveling outward from the bow shock that can be inferred from the foreshock wave boundary results of Diodato et al. (1976). Suitably oriented satellite proton detectors should be able to test the association between upstream waves and backstreaming particles and the apparent p-dependence along the shock by seeking the expected pattern statistically. The results of such a test should serve as a guide to investigation of the more complex actual morphology of foreshock particles and ultimately to analysis of wave-particle interactions upstream and to return particle production and emission processes in the quasi-parallel shock.

Acknowledgments. This study was funded in part by NASA Contract NASW-2877 and in part by TRW Independent Research and Development. The counsel of J. Benson was of great value.

References

Alfvén, H., and C. -G. Fälthammer, Cosmical Electrodynamics, Clarendon Press, Oxford, 1963.

Asbridge, J. R., S. J. Bame, and I. B. Strong, Outward flow of protons from the earth's bow shock, J. Geophys. Res., 73, 5777-5782, 1968.

Barnes, A., Theory of generation of bow-shock-associated hydromagnetic waves in the upstream interplanetary medium, Cosmic Electrodyn., 1, 90-114, 1970.

Benson, J., J. W. Freeman, H. K. Hills, and R. R. Vondrak, Bow shock protons in the lunar environment, The Moon, 14, 19, 1975.

Diodato, L., E. W. Greenstadt, G. Moreno, and V. Formisano, A statistical study of the upstream wave boundary outside the earth's bow shock, J. Geophys. Res., 81, 199-204, 1976.

Fairfield, D. H., Bow shock associated waves observed in the far upstream interplanetary medium, J. Geophys. Res., 74, 3451-3553, 1969.

Fredricks, R. W., A model for generation of bow-shock-associated upstream waves, J. Geophys. Res., 80, 7-17, 1975.

Greenstadt, E. W., Structure of the terrestrial bow shock, Solar Wind Three, Proc. of the Third Solar Wind Conf., Asilomar, Ed. C. T. Russell, Inst. Geophys. & Planet. Phys., UCLA, 440, 1974.

Greenstadt, E. W., The upstream escape of energized solar wind protons from the bow shock, The Magnetospheres of Earth and Jupiter, Ed. V. Formisano, D. Reidel Pub. Co., Dordrecht, Holland, 3, 1975.

Greenstadt, E. W., I. M. Green, G. T. Inouye, D. S. Colburn, J. H. Binsack, and E. F. Lyon, Dual satellite observation of the earth's bow shock. 3. Field-determined shock structure,

Cosmic Electrodyn., 1, 316-327, 1970.
Lin, R. P., C. -I Meng, and K. A. Anderson, 30- to 100-keV protons upstream from the earth's bow shock, J. Geophys. Res., 79, 489-498, 1974.
Spitzer, L., Jr., Physics of Fully Ionized Gases, Interscience, Wiley, New York, 1962.

(Received June 1, 1976;
revised July 19, 1976;
accepted July 30, 1976.)